IMPLEMENTATION OF AN MC-CDMA SYSTEM AND A STUDY ON WIRELESS CHANNEL MODELS

by

KRUTHIKA PONNUSAMY, B.E.

A THESIS

IN

ELECTRICAL ENGINEERING

Submitted to the Graduate Faculty
of Texas Tech University in
Partial Fulfillment of
the Requirements for
the Degree of

MASTER OF SCIENCE

IN

ELECTRICAL ENGINEERING

Approved

Tanja Karp
Chairperson of the Committee

Brian Nutter

Accepted

John Borrelli
Dean of the Graduate School

December, 2005

ACKNOWLEDGEMENTS

I dedicate my thesis work to my parents and sisters for their constant support and encouragement without which I could not have completed my education. I would like to express my sincere gratitude to the chairperson of my thesis committee, Dr. Tanja Karp. It was a great privilege to work with her. She has helped me a lot in understanding the concepts of multicarrier systems and its implementation. Her classes have instilled an immense interest in digital/wireless communications and I look forward to a successful career in the wireless industry.

I would like to thank Dr. Brian Nutter for being on my thesis committee. I would also like to thank Dr. Dean Fontenot, Dr. John Chandler and Mr. Eric Strong for their financial support and funding throughout my Master's program. I am deeply indebted to them for their faith in me and their support in times of need.

I would like to thank my close friends from Texas Tech University and my friends from the College of Engineering who helped me constantly throughout my Masters program. I would also like to thank my friends from Qualcomm for their support throughout my stay in the San Diego. Lastly, I would like to thank my wonderful nieces Tanu and Arya for their love and affection.

TABLE OF CONTENTS

LIST OF FIGURES

CHAPTER 1

INTRODUCTION

The market for the wireless industry has seen rapid growth in recent years. A lot of interest has been placed in modulation techniques like Orthogonal Frequency Division Multiplexing (OFDM) and Code Division Multiple Access (CDMA). OFDM is seen as a possible candidate for Fourth Generation (4G) wireless systems that demand higher data rates for voice and data transmissions. They also require more efficient performance in noisy macrocellular environments. A major outfall of the higher generation wireless systems is spectral efficiency.

CDMA is widely used in current Third Generation (3G) wireless systems. Spread spectrum technology, the underlying principle behind CDMA was popularly used in military communications for improved secrecy and low probability of interception during transmission. Today, CDMA is increasingly deployed in civilian markets thereby giving increased capacity and better performance.

Need for MC-CDMA

Narrowband communications is immune to Intersymbol Interference but susceptible to attenuation caused by fading. CDMA is characterized by resistance to fading by spreading the signal over the entire bandwidth. However, this is affected by delay spreads and thus inter-chip interference is seen as a major drawback.

OFDM is extremely popular in mobile communications over hostile radio environments. They use a large number of orthogonal parallel subcarriers for transmission. The biggest advantage of OFDM is the performance against intersymbol interference at the receiver and frequency selective fading. A large peak to average ratio and sensitivity to frequency offsets are seen as major drawbacks to OFDM.

MC-CDMA takes the advantages of both OFDM and CDMA and makes an efficient transmission system by spreading the input data symbols with spreading codes in the frequency domain. It uses a number of narrowband orthogonal subcarriers with symbol duration longer than the delay spread. This makes it unlikely for all the subcarriers to be affected by the same deep fades of the channel at the same time thereby improving performance. Synchronization during transmission becomes easier with longer symbol durations.

Thesis Overview

The objective of the thesis is to study and implement the Multicarrier CDMA system and study current macrocellular channel models. The MC-CDMA system uses CDMA spreading techniques before the application of the OFDM modulation technique. In the current implementation, the transmitter and receiver section of an MC-CDMA system is studied and implemented under ideal channel conditions. Since ideal conditions do not distort information during transmission, equalization techniques have been omitted from the implementation. A detailed literature search is also done on wireless channel models and popularly used channel models including Okumura-Hata Model, Longley-

Rice Model, Rayleigh Fading Channel Model and Ricean Fading Channel model are implemented in Matlab. Further research on this topic can be performed by introducing equalization techniques on the receiver end to mitigate channel effects on the MC-CDMA system.

The thesis is organized as follows. Chapter 2 gives a brief introduction to CDMA and OFDM. The OFDM transmitter and receiver section are implemented in Matlab for an ideal channel and an AWGN channel. In chapter 3, a basic study of the multicarrier modulation techniques is performed. The Multicarrier CDMA system is implemented in Matlab and studied. The receiver implementation is studied for an ideal channel. Chapter 4 is a detailed study of channel models. Macrocellular channel models Okumura-Hata and Longley-Rice channel are implemented in Matlab. Small scale fading models like Rayleigh and Ricean channel are studied and modeled in Matlab. The last chapter contains the results from the Matlab simulations.

CHAPTER 2

AN INTRODUCTION TO OFDM AND CDMA

Orthogonal Frequency Division Multiplexing (OFDM) is seen as a technique that uses parallel transmission of data through different subchannels that are orthogonal to each other thereby lowering the bit rate per carrier. In a conventional serial data system, the input data occupies the entire bandwidth during transmission. In a parallel data transmission system, multiple symbols are transmitted at the same time through the entire bandwidth. To ensure proper retrieval of data at the receiver end and to minimize interference, these parallel symbols are transmitted on orthogonal carriers in OFDM. The orthogonality of the subchannels allows the spectra of individual subchannels to overlap each other without any significant interference.

OFDM is seen as a useful multitone modulation or multiplexing scheme with multiple access capability, higher resistance to intersymbol interference (ISI) and improved performance over multipath fading channels.

Basic OFDM System

The transmitter section of the OFDM system is shown in Figure 1. The basic working principle of the OFDM is that a high bit rate input is split into parallel lower bit rates and transmitted across the channel. The use of parallel transmission effectively increases the symbol duration and reduces ISI considerably. OFDM uses orthogonal carrier frequencies to modulate input data. Orthogonality of the carrier frequencies

ensures that multiple-access is made possible in OFDM and thus each subcarrier carries unique information corresponding to the input data. It also cancels Inter-Carrier Interference (ICI). OFDM is the wireless counterpart to Discrete Multitone Modulation.

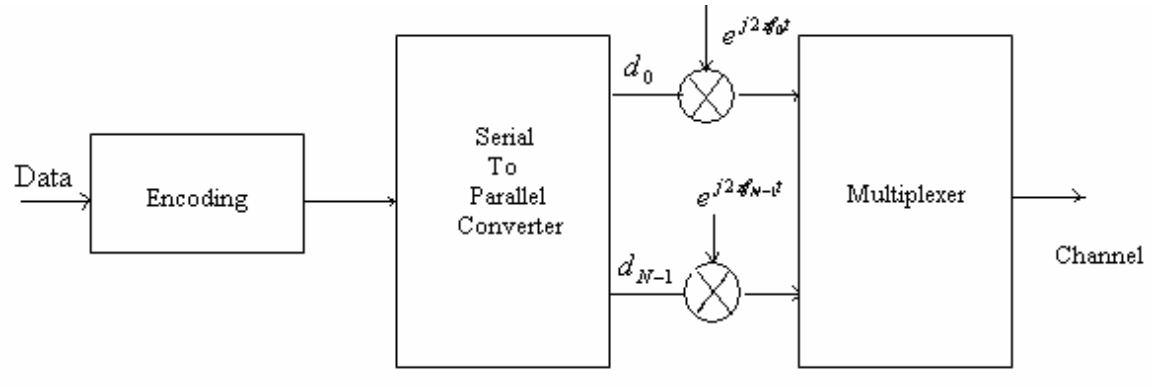

Figure 1 - Basic OFDM Transmitter System

A high bit rate data stream is divided into N parallel low bit data streams each at a rate of 1/N. Each data stream is modulated using different subcarriers (orthogonal carrier frequencies) in their respective subchannels. For signals to be orthogonal, they have to satisfy

$$\int_a^b \psi_p(t)\psi_q^*(t)dt = \begin{cases} k & \text{for } p = q \\ 0 & \text{for } p \neq q \end{cases} \qquad (2.1)$$

where * denotes the complex conjugate and the interval [a, b] is the symbol period.

By having these parallel data streams, the bandwidth of the modulation symbol is decreased by N or equivalently the time duration of the modulation symbol is increased by a factor of N. This can reduce ISI significantly.

To ensure orthogonality, if the symbol period is T, the frequency spacing should be 1/T.

The subcarrier frequencies are spaced as $f_n = f_0 + n\Delta f$ (2.2)

where $\Delta f = 1/N\Delta t$.

Pulse shaping methods (Rectangular Pulse Shaping in the case of OFDM) are employed to modulated signals in order to reduce the effects of ISI, reduce sensitivity to frequency and to minimize bandwidth requirements. Applying pulse shaping OFDM results in the subcarriers resembling sinc functions. This ensures that the sidebands of adjacent carriers overlap at zero crossings of the sinc function. This feature is shown in Figure 2 and 3 for OFDM systems.

The Inverse Fast Fourier Transform gives the Mathematical equivalent for pulse shaping. Thus, the IFFT of the modulated symbols is taken to obtain the required OFDM signal. Due to pulse shaping, the side lobes of the sinc functions are significant and there can be a lot of out-of-band interference. Also, pulse shaping requires that there is almost perfect frequency synchronization.

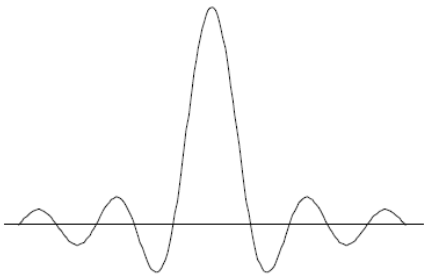

Figure 2 - Single Carrier of OFDM

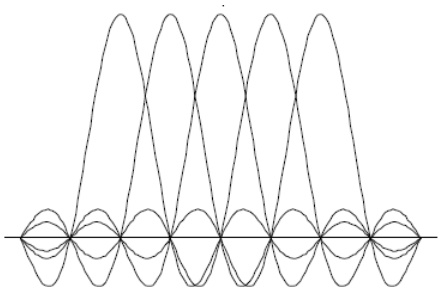

Figure 3 – Multiple carriers of OFDM

OFDM Transmitter

Implementation of the OFDM Transmitter as shown in Figure 6 involves the conversion of one stream of serial data to longer duration parallel data streams. These input bits are encoded and modulated depending on the system design and requirements. Different modulation techniques can be used in OFDM. Some of them are:

- Without Differential Encoding
  - M-QAM (Quadrature Amplitude Modulation)
  - M-PSK (Phase Shift Keying)
- With Differential Encoding
  - DPSK (Differential PSK)
  - DAPSK (Differential Amplitude PSK)

In order to remove ISI, a guard interval or cyclic prefix is added to the IFFT modulated data.

At the receiver end, the demodulation techniques available for the above modulation schemes are

- Coherent Demodulation of Nondifferential Modulation – The frequencies of each subcarrier should be synchronized or the phase offset is known to the system. Pilot carriers are used for synchronization purposes. In case of amplitude modulation techniques, attenuation of the subcarriers must also be known. For this type of demodulation, channel estimation is done at the receiver end. Some of the subcarriers are allocated to carry pilot symbols that contain transfer parameters for channel estimation. This means extra overhead for the system.
- Noncoherent Demodulation of Differential Modulation – This technique requires just the changes in the input to be known and recorded for demodulation. No pilot symbols are required which means lesser redundancy for the system.

Channel Coding techniques are used at the transmitter level of the OFDM system to improve SNR levels. They can be coherent or noncoherent depending on the modulation technique used. Simple systems use convolution coding and bit interleaving at the transmitter level and use the Viterbi algorithm for decoding at the receiver end. The Block diagram of a simple Coded OFDM system is given in Figure 4. Other complex techniques include Trellis Coded Modulation and Multilevel Coding.

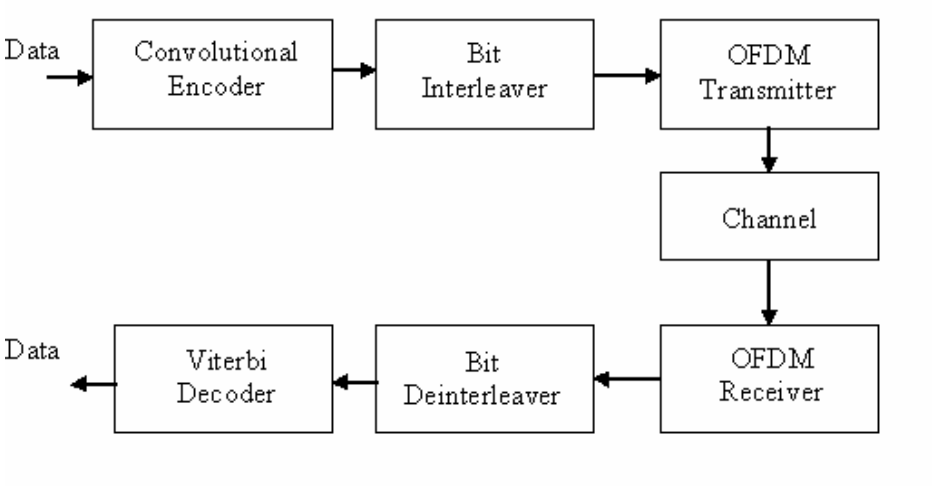

Figure 4 - Coded OFDM system

Synchronization

Frame synchronization is provided by adding zero blocks which contain no information. The receiver detects a new frame at the sight of every zero block. Time synchronization is provided by adding training sequences in addition to or instead of zero blocks.

The block diagrams for the current implementation of the OFDM transmitter and receiver sections are given in Figures 5 and 7.

Implementation of OFDM - Transmitter Section

A random number generator was used to obtain the digital data input and the number of subcarriers is decided for the implementation of the OFDM system.

QAM Modulation

The basic system has input that that goes to a QAM modulator whose outputs are the in-phase and quadrature components of the input. For convenience, a 16-QAM modulator is used. The input bits are sorted as groups of four bits each and if the number of input bits is not a multiple of 4, zeros are padded at the end of the input sequence. A complex symbol representing each group of four bits is obtained at the output of the QAM modulator and is mapped according to the points shown. For M-QAM, the values in the map are obtained from the array values for in-phase and quadrature components as

[-(sqrt (QAM_size) -1) * A: 2*A : (sqrt (QAM_size) -1) *A] (2.3)

where A is the scaling factor and 2 * A is the minimum distance between these points. Figure 6 shows the distribution of points in a 16-QAM modulated system.

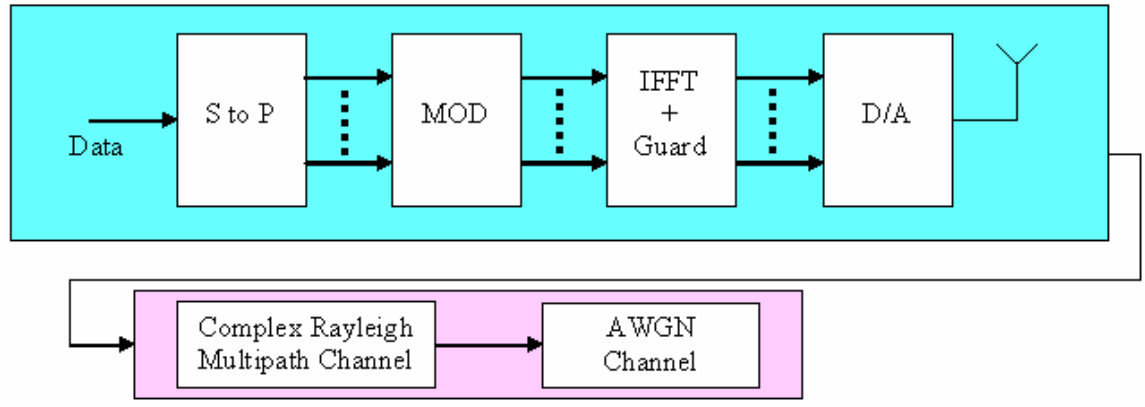

Figure 5 - OFDM Transmitter and Channel

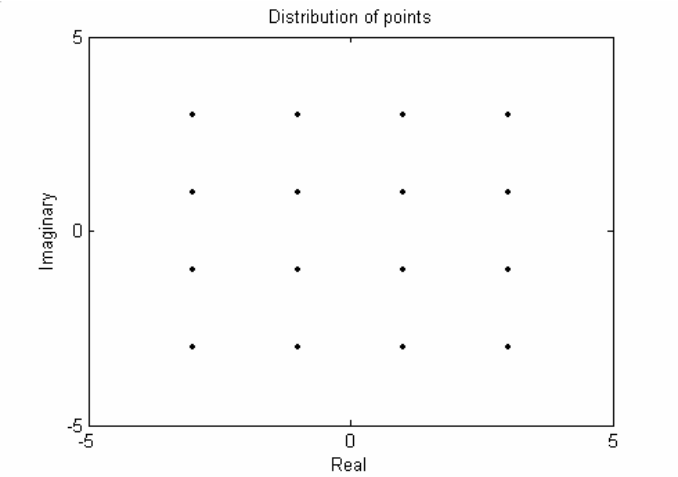

Figure 6 - Quadrature Amplitude Modulation

The average power of the symbols is calculated by taking the mean of the square of the absolute values of their complex values.

The IFFT of the complex symbols obtained as a result of QAM modulation is taken to obtain their time domain representation. In order to prevent ISI from affecting the output, a cyclic prefix of specific length is added to the IFFT modulated data. In the current implementation, the last part of the modulated data of required length is added at the beginning of the data to be transmitted. The parallel data from all the subcarriers is then converted into a serial row and transmitted through the channel. In practical situations, before sending the data to the channel, an up-conversion needs to be done. This is typically omitted in the simulation setup to improve speed.

Receiver Implementation

An exact inverse of the transmitter is performed at the receiving end. As the first step, the cyclic prefix is removed and sent to the FFT section. The FFT is performed to

obtain the signals in the frequency domain. A QAM demodulation is then performed to obtain the output data. The error between the transmitted and received data is calculated. For an ideal channel, it is noted that the error is negligible

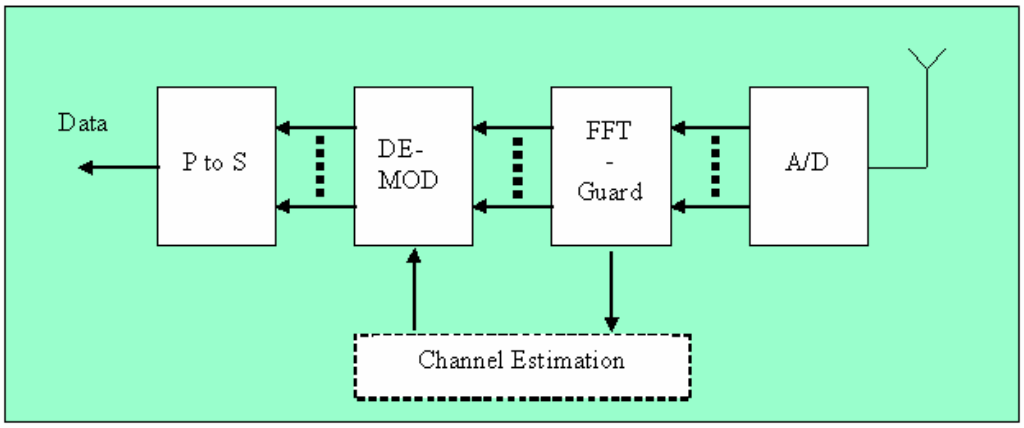

Figure 7 - OFDM Receiver

Code Division Multiple Access (CDMA)

CDMA is a digital technology that uses spread spectrum techniques to transmit information using the entire RF bandwidth. CDMA provides good capacity for voice and data transmissions.

Multiple access in CDMA is achieved by assigning users unique spreading sequences during transmission. Although all the users use the same 1.25MHz band for transmission, orthogonal codes provide a unique identity to each user that can be decoded at the receiver end. As the number of simultaneous users increases, system performance decreases due to interference from users within the system. Thus, capacity and quality of service are limited. Some of the major advantages of using CDMA include interference rejection, low probability of interception, fading rejection and secure transmission.

Features of CDMA

Power Control

The power seen by the handset is directly proportional to the distance between the transmitter and receiver. Thus, when a receiver is closer to the basestation, the power with which it transmits is much higher than the power of a receiver at the edge of the cell. This is seen as interference to the receiver farther from the transmitter and is called the near-far effect. In order to avoid or reduce interference caused by this effect, the receiver design includes power control measures that reduce the power with which it transmits to the basestation depending on the distance.

Handoff

Soft or Hard Handoff occurs when the mobile moving between cells is switching its cell station. At cell edges, the mobile tends to receive information from two or three neighboring basestations. The mobile performs continuous calculations of the SNR (signal to noise ratio) and decides to receive information from the basestation that transmits with maximum SNR. When switching from one basestation to the other, if the mobile disconnects with one basestation before linking to the other, it is called hard handoff. In most practical situations, at some point of time during switching, the mobile maintains a connection with more than one basestation. This is called soft handoff.

Rake receiver

The receiver in CDMA is based on the rake principle where multiple fingers receive the transmitted output and appropriate combining techniques (Maximal Ratio Combining or Equal Gain Combining) are used to process these multipath components.

CDMA Evolution

The application of Code Division Multiple Access (CDMA) technology was first introduced in cellular phones in the early 1990 with the IS-95 standard. Since then, increased capacity, high data rates, improved performance in harsh radio environments and other practical factors have played an important role in the need for successive new and improved standards. IS95-B was introduced in 1998 with enhancements to the existing standards including medium-rate packet data service, improved handoff performance and global roaming. The IS95 A/B standard based on 2G technology is popularly known as the cdmaONE standard.

Following this, the cdma2000 standardization took off aiming at IMT2000 (International Mobile Telecommunications) standards and backward compatibility with the existing cdmaONE networks and voice terminals. The IMT2000 standard has a globally acceptable spectrum for 3G systems including support for Time Division Duplex (TDD) and Frequency Division Duplex (FDD) modes.

Spreading

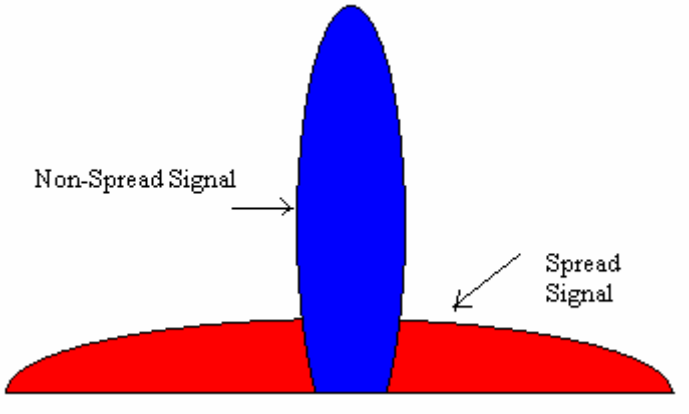

Figure 8 - Spreading Principle

Spread spectrum as shown in Figure 8 is a technique where the signal occupies the entire bandwidth for transmission. Direct Sequence spreading uses direct multiplication of the input sequence with a unique spreading code to avoid mutual interference between users in the system. These spreading codes are orthogonal to each other. Some common codes are Walsh Codes and Pseudo-Random Noise (PN) spreading codes. Spreading Factor is defined as the ratio between the chip rate and the data rate.

We restrict our study of CDMA to spreading techniques because of its relevance to MC-CDMA.

CHAPTER 3

MULTICARRIER CDMA

There is an increased urgency to define the next generation of Wireless Broadband Communication Systems. The rapid growth of video, voice and data transmission via the internet and the increased use of mobile telephony today have defined the necessity for higher data rate transmissions over the wireless channels. Though the current 3G systems use considerably higher data rates of 64kbps – 2Mbps as compared to 9.6kbps – 14.4kbps used by their 2G counterparts, the 4G systems that include broadband wireless services like High Definition Television (HDTV) require data rates up to 20Mbps. This also emphasizes the need for improved spectral efficiency and higher Quality of Service (QOS) over current systems.

The above requirements are seen as the primary driving force for more research on multicarrier modulation techniques. Single carrier systems give good data rates but are limited in performance in fading channels and any attempt to mitigate these effects results in an increased system complexity. Improved performance in bad channel conditions, high data rates and efficient bandwidth usage are the primary advantages of multicarrier modulation.

The major classification is based on spreading operation that takes place either in time or frequency domain. There are three types of multicarrier CDMA techniques.

- Multicarrier CDMA (MC-CDMA) Scheme
- Multicarrier Direct Sequence CDMA (MC DS-CDMA) Scheme

- Multitone CDMA (MT-CDMA) Scheme

Multicarrier DS-CDMA

The MC DS-CDMA system spreads the serial to parallel converted input stream in the time domain using the CDMA spreading code. The resulting data in the subchannels is orthogonal to each other with minimum frequency separation.

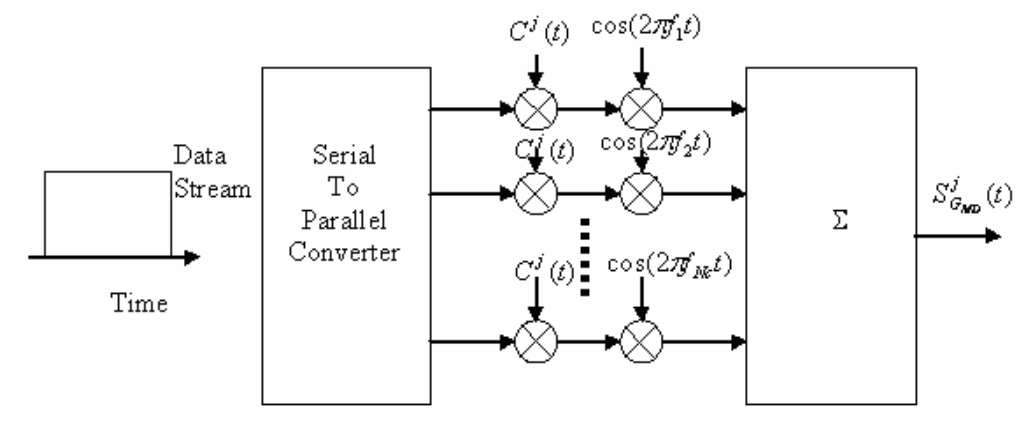

Figure 9 - Multicarrier DS-CDMA Transmitter

The transmitter section of an MC DS-CDMA system for the j[th] user is given in Figure 9. N_C denotes the number of subcarriers in the system and the spreading code for the j[th] user is given by $C^j(t) = [C_1^j C_2^j ....C_{G_{MD}}^j]$ in Figure 10. The power spectrum of the spread signal is given in Figure 11.

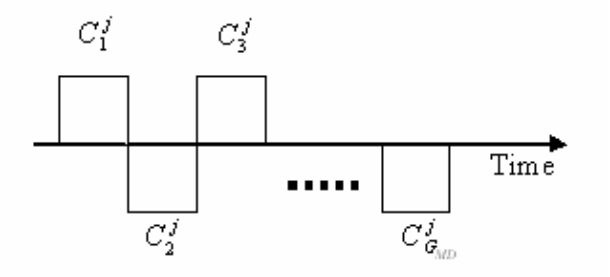

Figure 10 - Spreading Code in MC DS-CDMA

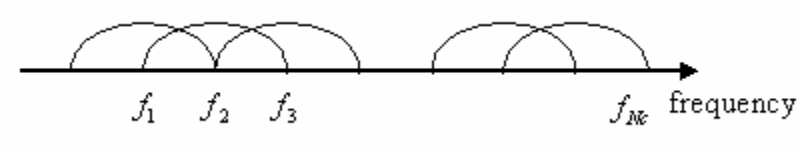

Figure 11 - Power Spectrum of the Transmitted Signal

The MC DS-DSMA system is ideally suited for uplink transmission.

Multitone CDMA

Parallel input data streams are spread using the CDMA spreading sequence in time domain and each subcarrier prior to spreading are orthogonal to each other. After spreading, the orthogonality condition is not satisfied in this case. The MT-CDMA system can accommodate a higher number of users than MC DS-CDMA because there are no restrictions with respect to the number of spreading codes and number of subcarriers. The spreading code for a Multitone CDMA system is shown in Figure 12.

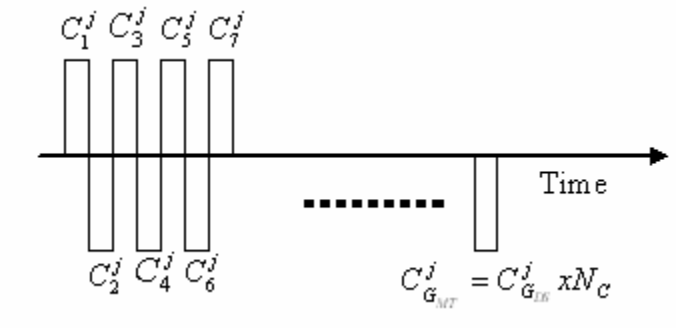

Figure 12 - Spreading Code for MT-CDMA system

Multicarrier CDMA

OFDM is an extremely successful technology in dealing with frequency selective fading and intersymbol interference. It is robust in multipath mobile environments and is tolerant to delay spreading. CDMA uses spreading a narrowband signal over a wide spectrum with a spreading sequence unique to each user. MC-CDMA combines the advantages of both OFDM and CDMA. The lower the symbol rate in each subcarrier, the longer the symbol duration and thus the easier to synchronize the transmissions.

The serial input data stream is converted into parallel streams and are spread using CDMA spreading sequences in the frequency domain. This ensures frequency non-selective fading in the subcarriers. This is shown in Figure 13 and the power spectrum of the signal is given in Figure 14.

The spreading of data symbols is represented as

$$s = \sum_{i=1}^{G_{MC}-1} d^{(i)}.c^{(i)} = (S_1, S_2 ... S_{G_{MC}})^T \qquad (3.1)$$

where $d^{(i)}$ is the input data for the ith user and $c^{(i)}$ is the spreading code for the ith user.

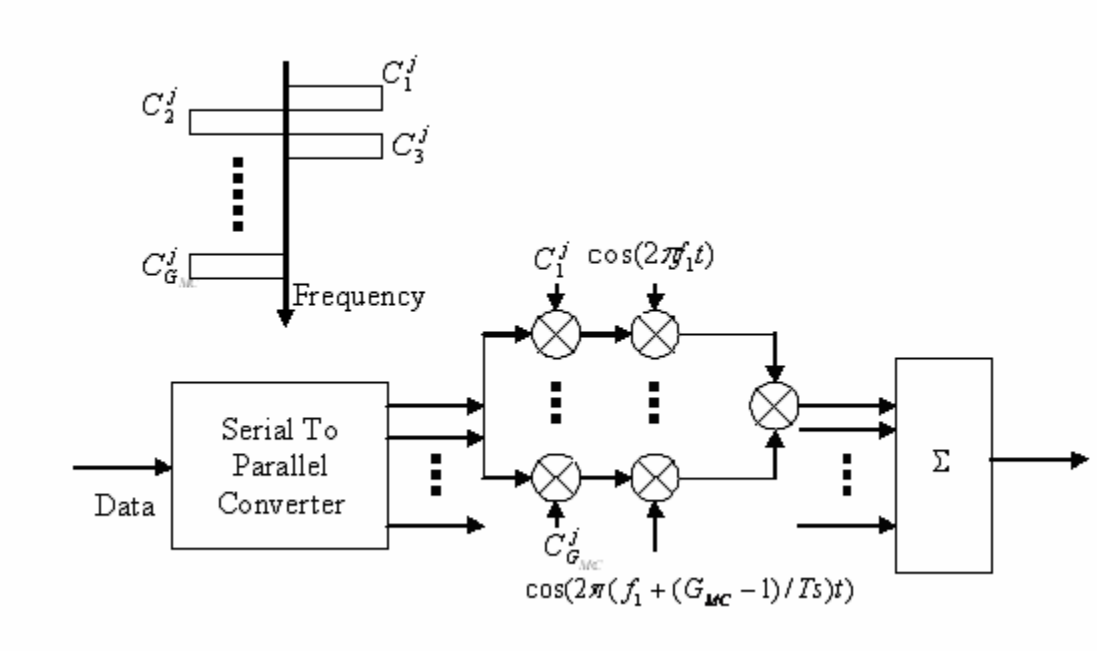

Figure 13 - Multicarrier CDMA Transmitter

The symbols S_l where l = 1 to G_{MC} are the component values of the subcarriers that are transmitted over the entire bandwidth using multicarrier modulation. The duration of each data symbol is T_s and the symbol duration T_c in each subcarrier after spreading is given by $T_c = T_s / L$ where L is the length of the spreading chip sequence or G_{MC}, the processing gain of the system.

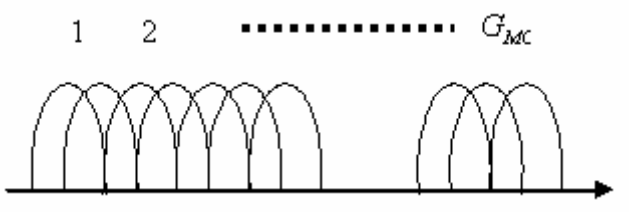

Figure 14 - Power Spectrum of MC-CDMA Signal

Transmitter Implementation

For a downlink cellular radio system, a block diagram for the transmitter section MC-CDMA system shown in Figure 15.

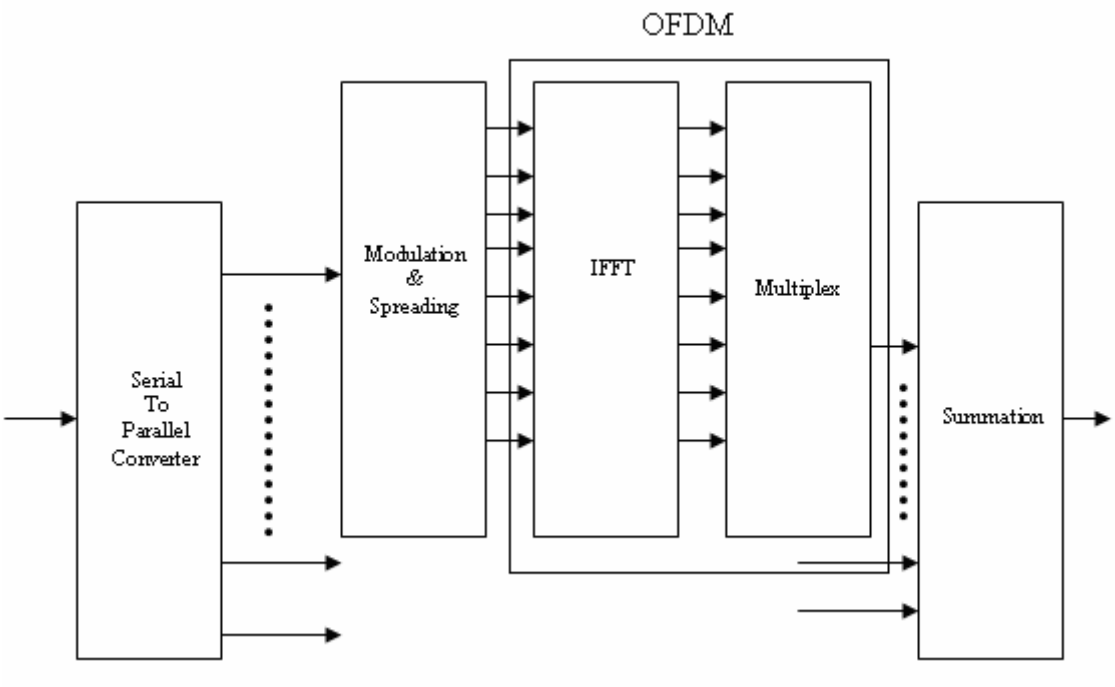

Figure 15 - MC-CDMA Transmitter Implementation

The transmitter section consists of an initial modulation scheme. The Quadrature Phase Shift Keying (QPSK) modulation technique is used in most practical situations. It is easy to implement and resilient to noise. Most satellite communication systems use QPSK for modulation.

Modulation

In QPSK, two bits of information are transmitted in each time slot. There are four possible phases ($\pi/4, 3\pi/4, 5\pi/4$ and $7\pi/4$) that can be allowed for transmission. The constellation diagram for QPSK is given in Figure 16.

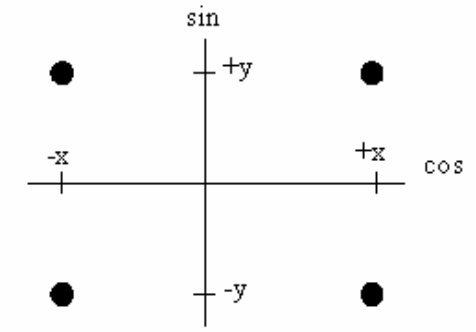

Figure 16 - QPSK Constellation

Spreading

Walsh-Hadamard sequences are bipolar spreading sequences that are used for channel separation in DS-CDMA. They are easy to generate, orthogonal sequences with zero crosscorrelation in ideal conditions. However, the correlation between sequences can increase due to delays/shift between them due to practical conditions. A basic Hadamard matrix is given by $\begin{bmatrix} +1 & +1 \\ +1 & -1 \end{bmatrix}$ and an N x N matrix is built from this basic matrix by repetition using the formula $H_{2N} = \begin{bmatrix} H_N & H_N \\ H_N & \overline{H}_N \end{bmatrix}$. (3.2)

Some of the important properties of walsh codes include

1. Zero cross correlation between the codes.
2. The scaled dot product of each code is 1.

3. The number of 1s and -1s are equal in each code sequence.

Multiplex and Summation

The chips after IFFT are summed and multiplexed to aligned before transmission through the channel.

Receiver Implementation

For an ideal channel environment, the receiver does a reverse of the transmitter implementation. The initial blocks are a reverse of the OFDM transmitter section followed by the despreading and demodulation of the output from there. After serial to parallel conversion, the received signal is multiplied by a gain $q_m^{j'}$ where *j* is the user, *m* is 1-G_{MC}. The decision variable $D^{j'}$ is calculated as

$$D^{j'} = \sum_{m=1}^{G_{MC}} q_m y_m \qquad (3.3)$$

where $y_m = \sum_{j=1}^{P} z_m^j d^j c_m^j$, the received signal envelope for the j^{th} user shown in Figure17.

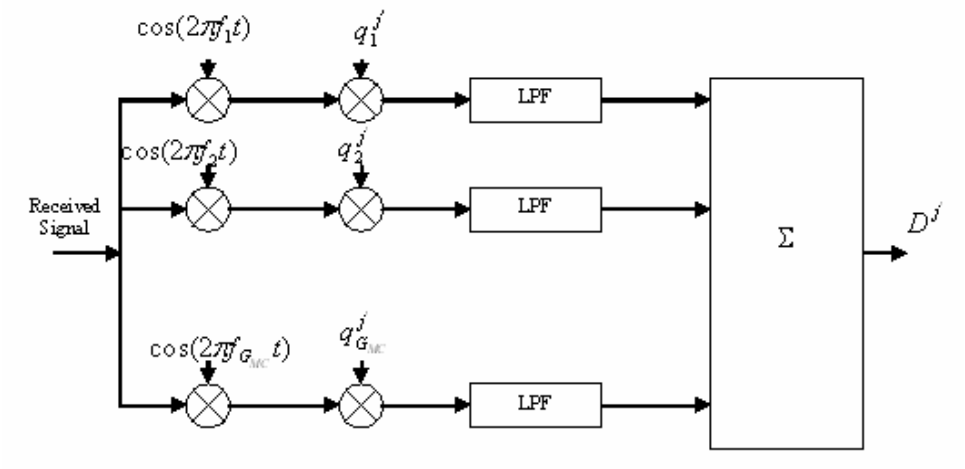

Figure 17 - Multicarrier CDMA Receiver

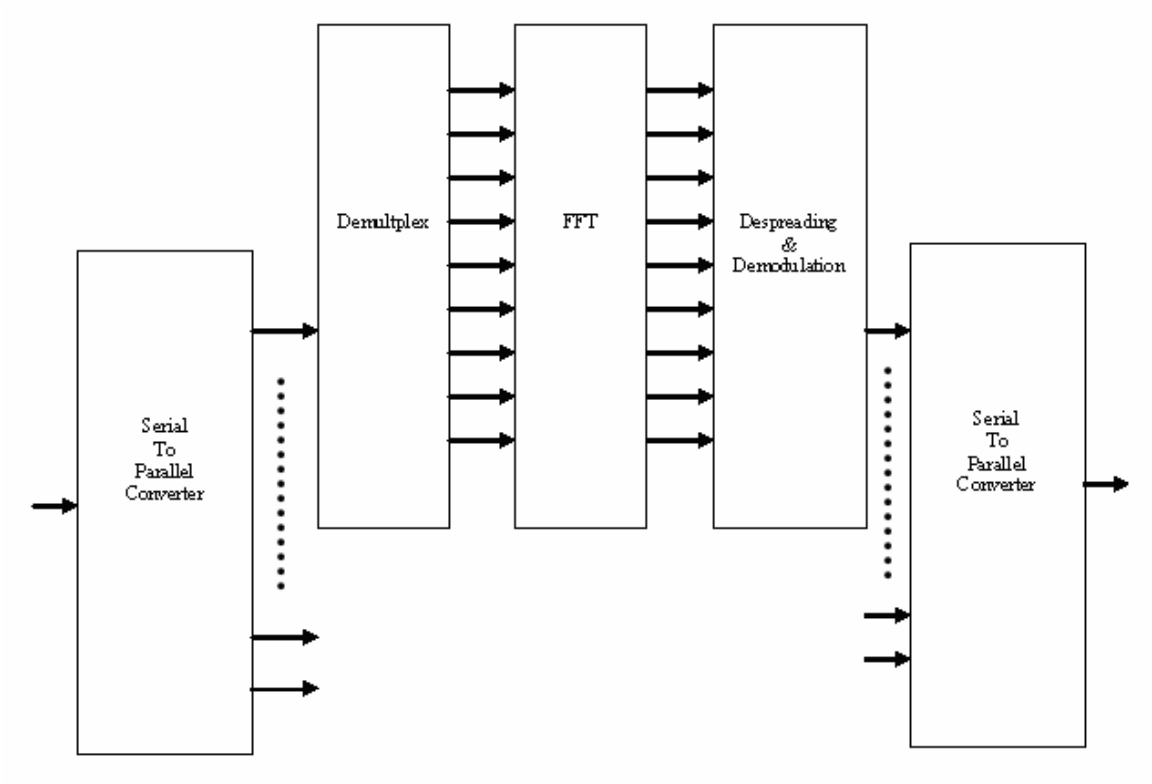

Figure 18 - MC-CDMA Receiver Implementation

An exact inverse of the transmitter is performed at the receiving end. As the first step, the cyclic prefix is removed and sent to the FFT section. The FFT is performed to obtain the signals in the frequency domain as shown in Figure 18.

Despreading Operation

Since the walsh code of the user is not known at the receiver section, a search operation is done where the received symbols are correlated to the walsh codes and the codes with maximum correlation with the received symbols are chosen.

CHAPTER 4

THE MOBILE RADIO CHANNEL

The nature of the radio channel affects the transmission of information through it. One of the major challenges facing engineers in mobile radio design has been modeling an accurate radio channel and its characteristics. Propagation models are broadly classified into two categories namely Large Scale Propagation and Small Scale Propagation models. They have been studied extensively to assess the effects of channels on the transmission and reception of signals in wireless conditions. Some common properties to be considered for channel design include fading, Doppler effect, diffraction, line of sight and propagation delay. Environmental properties affecting the radio channel include Urban/Hilly/Rural terrain, indoor/outdoor environment and weather conditions including humidity factor.

Depending on the received signal level, channels can have fast or slow fading. If the local average of signal varies slowly with displacement, large scale fading occurs. If there are rapid changes to the signal with small displacements, small scale fading occurs.

Depending on the frequency range, the radio channel types may vary. For a carrier frequency range between 3MHz-3GHz (Very High Frequency and Ultra High Frequency range), the radio channel is space wave dominant which contain ground waves and reflected waves (due to reflection and diffraction effects). This frequency range is used for FM radio and television channels.

Channel propagation models are either empirical or theoretical. Empirical or statistical models are based on experimental results but are usually not complete representations of channels and are hence not very accurate. These models are used to predict macrocell environments. Theoretical or deterministic models lack computational efficiency and are used to model microcell or indoor propagation models. The idealized image for wireless channels is the AWGN model. This is not possible in reality where there are numerous external factors affecting the channel performance.

Definition of Cell Types

Depending on the radio environment, propagation models can be outdoor or indoor models. Outdoor models are further classified as macrocell and microcell models. Cell types are classified depending on the cell radius. Macrocells(large cells) have a typical cell radius of 1km to 30 km, microcells have upto 1 km cell radius, and picocells have a radius of up to 500m. A typical macrocellular propagation model is in Figure 19.

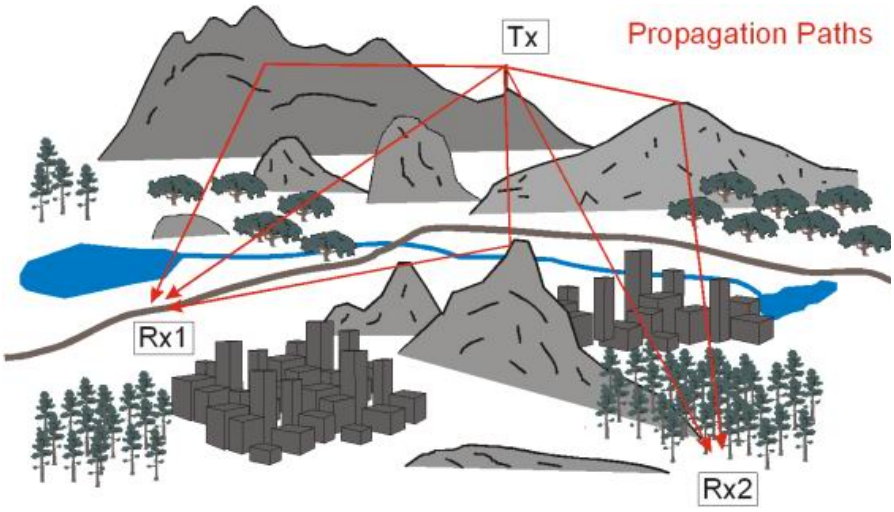

Figure 19 - Typical Macrocellular Propagation Model

For accurate frequency planning, one of the most important characteristics required to be known is the propagation loss. Free space path (propagation) loss is the signal degradation caused due to signal spreading as the distance between the source and the destination increases.

The free space received power is given by the Friis Free Space Equation

$$P_r(d) = P_t.G_rG_t\left(\frac{\lambda}{4\pi.d}\right)^2 \quad (4.1)$$

where P_t is the transmitter power, G_r is the receiver antenna gain, G_t is the transmitter antenna gain, λ is the wavelength and d is the distance between the transmitter and the receiver. This shows that the received power falls off as the square of the T-R separation. The path loss in free space is given by $\frac{P_r}{P_t}$.

Propagation in a wireless environment is affected by diffraction, scattering, reflection and refraction as shown in Figure 20. The final received signal is usually a sum of all the components of these effects. It is very difficult to model a wireless channel accurately because of the various factors influencing the channel.

Reflection of signals takes place when the signal from the transmitter does not reach the receiver directly. Instead, the signal reflects over surfaces, buildings and other obstacles before reaching the receiver. Signals thus received have a shifted phase and either increase or decrease the signal level depending on constructive or destructive interference of the signals. This is commonly referred to as multipath fading where multiple components of the signal are received at the receiver section with shifted phase.

The incident and reflected signals are related by the Fresnel Reflection Coefficient (Γ) which depends angle of incidence, frequency and polarization. Depending on the presence of a line of sight component, these signals are further classified as Rayleigh or Ricean distributed.

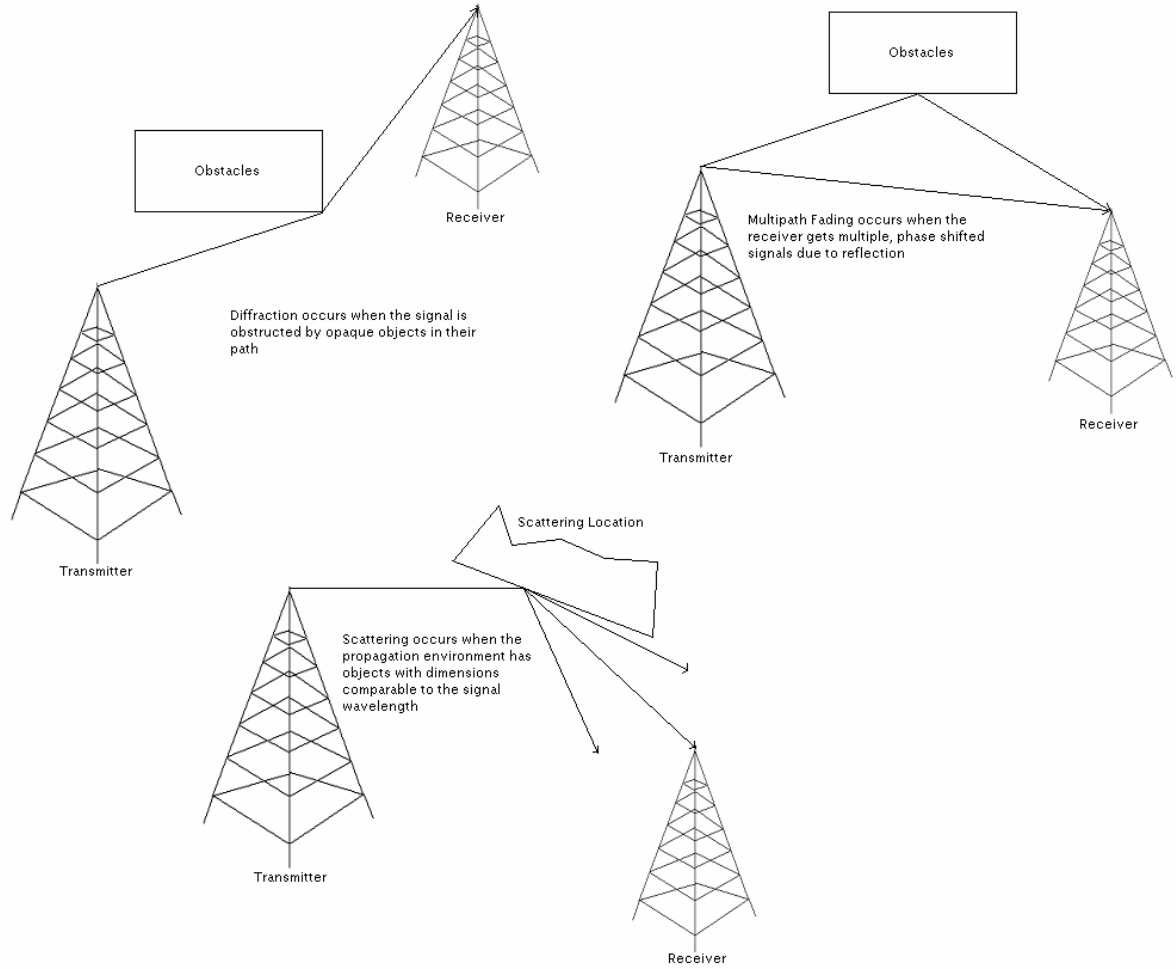

Figure 20 - Diffraction, Reflection and Scattering

Diffraction is the bending of signal around opaque obstacles whose dimensions are significantly larger than the signal wavelength. This is explained using Huygens principle which states that all points on a wavefront can be regarded as a new source of secondary wavelets, and these wavelets produce a new wavefront in the direction of

propagation. At the obstacle edges, attenuation occurs due to diffraction because the radio signals are scattered. Diffraction is usually seen in non line of sight conditions.

Depending on the environment, the signal scattering during transmission varies. Scattering occurs when the radio waves impinge on uneven surfaces and as a result of this, the energy gets reflected or scattered. This modeling is similar to diffraction but there is a higher number of secondary wavelets in scattering. Due to this reason, it is more difficult to model scattering.

Refraction plays a major role when transmission is across greater distances. The refractive index of the atmosphere is not constant and this contributes to the bending of waves.

Empirical Propagation models for Macrocell Environment

Mobile Channel Environment is characterized by irregular terrain. Also, in large cells, LoS conditions are usually not satisfied. Accurate large scale models must take terrain features (hilly, moderate or flat) into consideration. The model is also dependent on base station and receiver antenna height. This has been one of the major areas of research and there are a large number of models today. Models are usually based on rms delay spread values, antenna gain reduction factors or the presence of LoS components.

Okumura-Hata Model

In the present Engineering scenario, Okumura-Hata is the most widely used for UHF and VHF land-mobile radio systems. This model is completely based on measured

data and has no scope for analytical explanation. Practical implementation of the model requires extensive data gathering. Okumura developed a set of curves giving attenuation relative to free space. Most of the data collected for this model was based on the terrain in and around Japan. The result from this data is has been compiled into diagrams from which appropriate measurements can be made. Hata approximated these curves into formulae and gave an empirical definition to these models. He also brought in correction factors to accommodate the terrain conditions.

The Okumura-Hata model is valid in a frequency range of 150-1000MHz for a transmitter-receiver distance of upto 20km. The path loss in dB is given by

$$A[dB] = 69.55 + 26.16 * \log(f[MHz]) - 13.82 * \log(h_{Tx}[m]) + (44.9 - 6.55 * \log(h_{Tx}[m])) * \log(d[km]) - \beta, \quad (4.2)$$

where f is the frequency in MHz, h_{Tx} is the transmitter height in *m*, *d* is the distance between the transmitter and receiver in *km* and β is the correction factor.

$$\beta_{urban} = \begin{cases} [1.1 * \log(f[MHz]) - 0.7] * h_{Rx}[m] - [1.56 * \log(f[MHz]) - 0.8], & \text{for small cities} \\ 8.298[\log(1.54 * h_{Rx}[m])]^2 - 1.1, & \text{for urban areas and } f \le 300\text{MHz} \\ 3.2 * [\log(11.75 * h_{Rx}[m])]^2 - 4.97, & \text{for urban areas and } f \ge 300\text{MHz} \end{cases} \quad (4.3)$$

where h_{Rx} is the height of the receiver antenna in *m* and β_{urban} is the correction factor for urban environment. For three further environments including suburban and rural areas, a correction factor is further added to this urban value.

$$\beta_{new} = \begin{cases} \beta_{urban} - 2*[\log(f[MHz]/28)]^2 - 5.4, \\ \qquad\qquad \text{, for suburban areas} \\ \beta_{urban} - 4.78*[\log(f[MHz])]^2 + 18.33*\log(f[MHz]) - 35.94, \\ \qquad\qquad \text{, for almost open rural areas} \\ \beta_{urban} - 4.78*[\log(f[MHz])]^2 + 18.33*\log(f[MHz]) - 40.94, \\ \qquad\qquad \text{, for open rural areas} \end{cases} \tag{4.4}$$

This model is extended by COST (European Co-operative for Scientific and Technical Research) to form the COST 231-Hata model for frequencies between 1500MHz and 2000MHz.

$$A[dB] = 46.3 + 33.9*\log(f[MHz]) - 13.82*\log(h_{Tx}[m]) + 44.9 - 6.55*\log(h_{Tx}[m])]*\log(d[km]) - \beta + \begin{cases} 3, & \text{for big city center} \\ 0, & \text{other cases} \end{cases} \tag{4.5}$$

$$\beta = [1.1*\log(f[MHz]) - 0.7*h_{Rx}[m] - [1.56*\log(f[MHz]) - 0.8] \tag{4.6}$$

The disadvantages include the inability to use these curves to extrapolate values for specific situations.

Longley-Rice Model

Anita Longley and Phil Rice modeled the channel for frequencies between 20MHz and 20GHz. This model operates in two modes namely the area prediction mode and the point to point mode. It is also popularly known as the ITS Irregular Terrain Model.

The Longley – Rice model predicts the reference attenuation A_{ref} , a function of distance *d*. The variables used to model this channel are

d	Distance between the two terminals
h_{g1}, h_{g2}	Transmitter and Receiver Antenna Heights
k	Wave number
Δh	Terrain Irregularity Parameter
N_s	Mean Surface Refractivity measured in N—units
γ_e	Earth's Effective curvature in units of reciprocal length
Z_g	Surface Transfer Impedance of the ground

Wave number *k* is defined as $2\pi / \lambda = f / f_o$ with $f_o = 47.70 MHz.m$, λ is the wavelength and *f* is the frequency in MHz.

Surface Refractivity is given by $N_s = N_o e^{-0.1057 z_s}$ (4.7)

where N_o is the surface refractivity at sea level, and z_s is the elevation of the surface above mean sea level in kilometers. The earth's effective radius is required to represent the transmission of the signal through a straight line for the first kilometer. It is given by the empirical formula

$\gamma_e = \gamma_a [1 - 0.04665 e(0.005577 N_s)]^{-1}$ (4.8)

where γ_a is the earth's actual curvature and is taken to be 6370 km.

The terrain irregularity parameter Δh is the roughness factor associated with different terrain profiles. The roughness factor is the interdecile range of terrain heights in meters above and below a straight line fitted to the average slope of the terrain. In the absence of this value, standard values are used for the roughness factor depending on the terrain as shown in table 1.

Table 1 - Terrain Roughness Factor

Type of Terrain	Δh in meters
Water or very smooth terrain	0-1
Smooth terrain	10-20
Slightly rolling terrain	40-60
Hilly terrain	80-150
Rugged mountains	200-500

The surface transfer impedance is defined as

$$Z_g = \begin{cases} \sqrt{\varepsilon_r' - 1} & \text{Horizontal polarization} \\ \sqrt{\varepsilon_r' - 1/\varepsilon_r'} & \text{Vertical polarization} \end{cases} \tag{4.9}$$

where ε_r' is the complex relative permittivity defined by $\varepsilon_r' = \varepsilon_r + iZ_o\sigma/k$, ε_r is the relative permittivity, σ is the conductivity of the ground in siemens per meter, and $Z_o = 376.62$ ohm.

The reference attenuation A_{ref} is given by the piecewise formula

$$A_{ref} = \begin{cases} \max(0, A_{el} + K_1 d + K_2 \ln(d/d_{Ls})) & d \le d_{Ls} \\ A_{ed} + m_d d & d_{Ls} \le d \le d_x \\ A_{es} + m_s d & d_x \le d \end{cases} \tag{4.10}$$

where the coefficients A_{el}, A_{ed}, and A_{es} are the attenuation components due to line of sight component, diffraction and scattering respectively. The values of the other

coefficients vary depending on the three attenuation component calculations and are given below.

Initial Calculations for L-R model

Angular distance θ is given in radians by

$$\theta = \theta_{et} + \theta_{er} + d/\gamma_e \tag{4.11}$$

where $\theta_{ej} = [0.65 * \Delta h(d_{Lsj}/d_{Lj} - 1) - 2h_{ej}]/d_{Lsj}$ is the angle by which the horizon rays are elevated or depressed relative to the horizontal at each antenna *j* varying between *t* and *r* for transmitter and receiver antenna,

$$d_{Lj} = d_{Lsj} e[-0.07\sqrt{\Delta h / \max(h_{ej}, H3)}] \tag{4.12}$$

is the distance of the transmitter and receiver from the horizontal obstacle to the antenna, H3 = 5m, $d_{Lsj} = \sqrt{2h_{ej}/\gamma_e}$, *j* is either for transmitter or receiver.

$d_{Ls} = d_{Lst} + d_{Lsr}$ and $d_L = d_{Lt} + d_{Lr}$ and effective angular distance

$$\theta_e = \max(\theta_{et} + \theta_{er}, -d_L\gamma_e)\,. \tag{4.13}$$

Diffraction Attenuation

The model takes into account the rounded earth attenuation, double knife edge attenuation and clutter components into account. The diffraction attenuation A_{ed} depends on $d, d_{Lj}(d_{Lt}, d_{Lr})$, N_s, terrain roughness factor Δh, and the sum θ_e of the elevations θ_{et} and θ_{er} of rays above the horizontal of each antenna.

Total diffraction attenuation is given as

$$A_{diff}(d) = (1-w)A_k + wA_r + A_{fo} \tag{4.14}$$

where A_k is the double knife edge attenuation, A_r is the rounded earth attenuation and A_{fo} is the clutter factor due to absorption and scattering by oxygen, water vapor, precipitation and terrain clutters.

The weighting factor *w* is given by

$$w = \frac{1}{1+0.1\sqrt{Q}} \tag{4.15}$$

with $Q = \left[1+0.045\left(\frac{\Delta h}{\lambda}\right)^{\frac{1}{2}}\left(\frac{\gamma_a\theta + d_L}{d}\right)^{\frac{1}{2}}\right]^{-1}$.

Double Knife Edge Attenuation A_k is given by

$$A_k = Fn(v_t) + Fn(v_r) \tag{4.16}$$

where *Fn(v)* is defined by the Fresnel Integration $Fn(v) = 20\log\left|\frac{1}{\sqrt{2i}}\int_v^{\infty} e^{i\pi u^2/2}du\right|$ and

$v_j = \frac{\theta}{2}\left(\frac{k}{\pi}\frac{d_{Lj}(d-d_L)}{d-d_L+d_{Lj}}\right)^{\frac{1}{2}}$, j = *t* for transmitter and *r* for receiver.

Rounded Earth Attenuation A_r is given by

$$A_r = G(x_0) - F(x_t, K_t) - F(x_r, K_r) - C_1(K_0) \tag{4.17}$$

In order to calculate a solution for this one, Vogler's formulation uses the three radii method.

$\gamma_0 = \theta/(d-d_L)$ and $\gamma_j = 2h_{ej}/d_{Lj}^2$, j = *t* for transmitter and *r* for receiver.

$\alpha_j = (k/\gamma_j)^{1/3}$, *j=0, t* and *r*.

K_j are complex numbers defined as $K_j = \dfrac{1}{i\alpha_j Z_g}$, *j=0, t* and *r*.

$x_0 = AB(K_0)\alpha_0\theta + x_t + x_r$ where $x_j = AB(K_j)\alpha_j\gamma_j d_{Lj}$, *j* = *t* and *r* for transmitter and receiver. A is a dimensionless constant given by 151.03.

For the spherical earth problem, Vogler's formulation solution introduces a special function

$$W_i(z) = A_i(z) + iB_i(z) \tag{4.18}$$

whose solution is given by

$$W_i(t_0) = 2^{1/3} K W_i^{'}(t_0) \tag{4.19}$$

from which the value for *B* is obtained as

$$B = 2^{-1/3}\,\mathrm{Im}\{t_0\} \tag{4.20}$$

$$G(x) = 20\log(x^{-1/2}e^{x/A}) \tag{4.21}$$

$$F(x,K) = 20\log\left|(\pi/(2^{1/3}AB))^{1/2} W_i(t_0 - (x/(2^{1/3}AB))^2)\right| \tag{4.22}$$

$$C_1(K) = 20\log\left|\frac{1}{2}(\pi/(2^{1/3}AB))^{1/2}(2^{2/3}K^2 t_0 - 1)W_i^{'}(t_0)^2\right| \tag{4.23}$$

Distances d_3 and d_4 are calculated using the formulae

$$X_{ae} = (k\gamma_e^2)^{-1/3} \tag{4.24}$$

$$d_3 = \max(d_{Ls}, d_L + 1.3787 X_{ae}) \tag{4.25}$$

and $d_4 = d_3 + 2.7574 X_{ae}$. (4.26)

$$A_3 = A_{diff}(d_3) \text{ and } m_d = (A_4 - A_3)/(d_4 - d_3) \tag{4.27}$$

and total diffraction attenuation is given by

$$A_{ed} = A_3 - m_d d_3 \tag{4.28}$$

Line of Sight Attenuation

Line of sight attenuation is given by

$$A_{el} = A_2 - K_1 d_2 \tag{4.29}$$

The calculations required for this are obtained from below.

$$d_2 = d_{Ls},\ A_2 = A_{ed} + m_d d_2 \tag{4.30}$$

If $A_{ed} \geq 0$, $d_0 = \min(\frac{1}{2} d_L, 1.908 k h_{et} h_{er})$, $d_1 = \frac{3}{4} d_0 + \frac{1}{4} d_L$ from where we calculate

$$A_0 = A_{los}(d_0) \tag{4.31}$$

and $A_1 = A_{los}(d_1)$ (4.32)

$$K_2^{'} = \max\left[0, \frac{(d_2 - d_0)(A_1 - A_0) - (d_1 - d_0)(A_2 - A_0)}{(d_2 - d_0)\ln(d_1/d_0) - (d_1 - d_0)\ln(d_2/d_0)}\right]$$

$K_1^{'} = (A_2 - A_0 - K_2^{'} \ln(d_2/d_0))/(d_2 - d_0)$.

If $K_1^{'} \geq 0$, $K_1 = K_1^{'}$ and $K_2 = K_2^{'}$.

However, if $K_1^{'} < 0$, $K_2^{''} = (A_2 - A_0)/\ln(d_2/d_0)$ and if $K_2^{''} \geq 0$, $K_1 = 0$ and $K_2 = K_2^{''}$.

Otherwise, $K_1 = m_d$, $K_2 = 0$.

If $A_{ed} < 0$,

$$d_0 = 1.908 k h_{et} h_{er} \tag{4.33}$$

$$d_1 = \max(-A_{ed} / m_d, d_L / 4) \tag{4.34}$$

If $d_0 \geq d_1$ or $K_2^{'} = 0$, $K_1^{''} = (A_2 - A_1)/(d_2 - d_1)$. If $K_1^{''} > 0$, $K_1^{'} = K_1^{''}$, and $K_2 = 0$ else

$K_1 = m_d$, $K_2 = 0.$

Attenuation caused due to line of sight is calculated from the formula

$$A_{los}(d) = (1 - w)A_d + wA_t \tag{4.35}$$

where $A_d = A_{ed} + m_d d$ (4.36)

is the extended diffraction attenuation and the two-ray attenuation is given by

$$A_t = -20 \log\left|1 + R_e e^{i\delta}\right| \tag{4.37}$$

For two-ray attenuation, we have $\sin\psi = \dfrac{h_{et} + h_{er}}{\sqrt{d^2 + (h_{et} + h_{er})^2}}$ and

$$R_e^{'} = \begin{cases} \dfrac{\sin\psi - Z_g}{\sin\psi + Z_g} \exp[-k\sigma_h(s)\sin\psi] & \text{if } \left|R_e^{'}\right| \geq \max(1/2, \sqrt{\sin\psi}) \\ \text{otherwise} \end{cases}.$$

$$R_e = \begin{cases} R_e^{'} \\ (R_e^{'} / \left|R_e^{'}\right|)\sqrt{\sin\psi} \end{cases}$$

We also have $\delta^{'} = 2kh_{et}h_{er} / d$ and $\delta = \begin{cases} \delta^{'} & \text{if } \delta^{'} \leq \pi/2 \\ \pi - (\pi/2)^2 / \delta^{'} & \text{otherwise} \end{cases}$

Scattering Attenuation

Distances are defined as

$$d_5 = d_L + D_d \tag{4.38}$$

$$d_6 = d_5 + D_d \tag{4.39}$$

where $D_d = 200km$.

$$A_5 = A_{scat}(d_5) \tag{4.40}$$

$$A_6 = A_{scat}(d_6) \tag{4.41}$$

where $A_{scat}(d)$ gives the scattering component of attenuation over distance d. A_5 and A_6 are undefined sometimes in which case $d_x = +\infty$ and A_{es}, m_s is also undefined.

$$m_s = (A_6 - A_5)/D_s \tag{4.42}$$

$$d_x = \max[d_{Ls}, d_L + X_{ae}\log(kH_s), (A_5 - A_{ed} - m_s d_5)/(m_d - m_s)] \tag{4.43}$$

$$A_{es} = A_{ed} + (m_d - m_s)d_x \tag{4.44}$$

where $H_s = 47.7m$.

Angular distance θ is given by $\theta = \theta_e + \gamma_e d$. $\theta' = \theta_{et} + \theta_{er} + \gamma_e d$ and $r_j = 2k\theta' h_{ej}$, j is t and r for transmitter and receiver.

If r_t and r_r are less than 0.2, attenuation in the scattering region is undefined or infinite. Otherwise,

$$A_{scat}(d) = 10\log(kH\theta^4) + F(\theta d, N_s) + H_0 \tag{4.45}$$

where H_0 is the frequency gain function.

Thus the total attenuation is calculated after taking the above factors into consideration. Other Channel models are given below.

Ericsson Model 9999

Based on the Okumura-Hata Model, this is used in the cellular system specifically for GSM, PCS etc.

Clearance Angle Method

This method is used in Digital Mobile systems like GSM, Paging and old analog systems. It has a simple implementation with good prediction accuracy. It predicts both rural and urban environments in the VHF and UHF range.

Lee Model

Used extensively in the US, this model is used in various radio systems (AMPS, IS-95). It consists of two parts. Area-to-area prediction is used for flat terrains and point-to-point prediction takes hilly terrain into consideration. In the absence of LoS conditions, the obstructions are modeled as knife-edges and diffracted waves are computed.

A list of channel model for the various frequency ranges are shown in Figure 21.

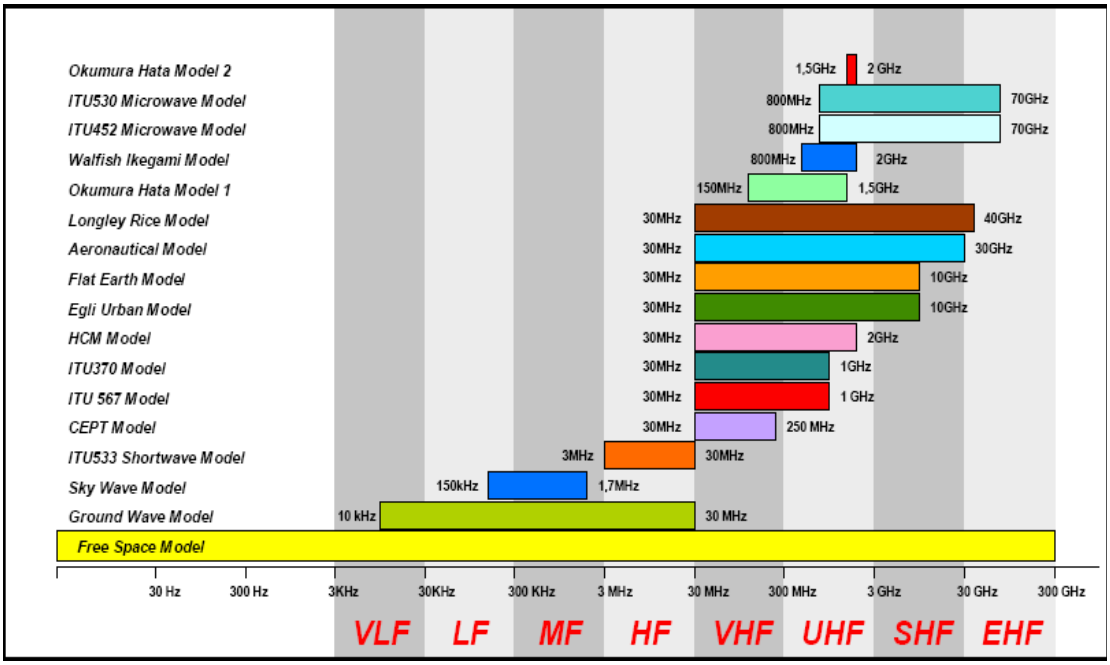

Figure 21 - Channel Models for appropriate frequency ranges

ANN (Artificial Neural Network) Models

This works on a feed-forward neural network architecture. It has shown very good performance with accurate predictions and computational ease. It is used in 450MHz and 900 MHz frequency range.

Empirical Propagation models for Microcell Environment

The main assumptions are smaller antenna height, short radio paths and low transmitting power.

Two-Ray Model

One of the most elementary models for microcell environments, this model is used for a LoS radio channel. The received signal is the sum of each ray reaching the

antenna. But there are more complex models to deal with a large number of rays like four-ray and six-ray model.

Corner Diffraction is an important effect that is considered in Uniform Theory of Diffraction Model. A quasi 3D UTD model is popularly used. It takes into account multiple reflections and diffraction components.

Indoor Propagation Models

Depending on path amplitudes, channels models are subject to multipath propagation, shadowing & fading effects. Multipath reception channels can be modeled as Rayleigh or Ricean fading channels. These are called small-scale effects. In the presence of a significant Line of Sight component, the channel model is Ricean and when there is no Line of sight component, the channel follows a Rayleigh distribution. The Lognormal distribution is used in a large number of cases. Multiple reflections in a multipath environment cause the fading effects to be a multiplicative process giving rise to a lognormal distribution. In multicarrier operation, this results in different attenuation at different subcarriers or at different locations. Presence of Doppler Spread also affects the model behaviour. The most popular models are the ray-tracing and Finite-Difference Time-Domain models.

Ray-tracing method is one of the most accurate field strength prediction model. Though they are computationally complex, ray-tracing algorithms quite successfully predict the channels.

Finite-Difference Time-Domain (FDTD) method is one of the most popular numerical solution. Similar to the ray-tracing method, they are computationally demanding.

Small Scale Propagation Models

Small Scale Propagation models predict the fluctuations in the received signal strength which is the sum of many signals affected due to various reflections reaching the receiver over a very short period of time. It is also caused due to the presence of more than a single component of the transmitted signal at the receiver end. The resultant of these multipath components varies in delay, phase and amplitude. Fading is classified into different types. Based on the multipath time delay spread, fading can be flat or frequency selective and depending on Doppler spread, they can be fast or slow fading.

Flat fading occurs when the bandwidth of the signal is smaller than the bandwidth of the channel. It is sometimes known as amplitude varying channels or narrowband channels. In flat fading, the delay spread is also less than the symbol period. Flat fading channels are modeled as Rayleigh or Ricean distributed channels.

When the delay spread is greater than the symbol period, there are multiple versions of the transmitted signal at the receiver. When this happens, the received signal is attenuated and differs in phase. This is called Frequency Selective Fading. The bandwidth of the symbol is greater than the bandwidth of the channel. This causes Intersymbol Interference (ISI). These channels are widely known as wideband channels

and are modeled as Two-Ray Rayleigh models. A gist of small scale fading classification is given in figure 22.

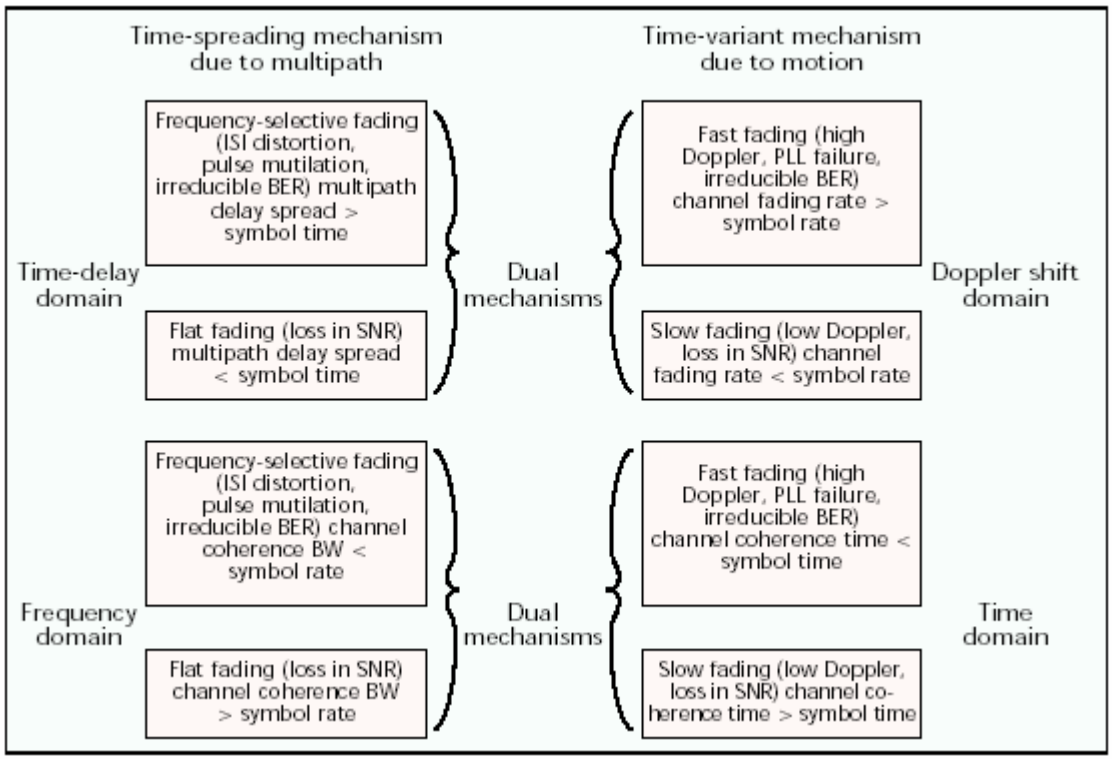

Figure 22 - Small Scale Fading

Factors contributing to small scale fading include multipath propagation, mobile velocity, and the transmission bandwidth of the signal.

Multipath Propagation is caused due to reflection/scattering of transmitted signals. Doppler Shift is the frequency shift in the received signal caused due to the relative motion between the transmitter and the receiver. This phase change is given by

$$f_d = (v/\lambda).\cos\theta \qquad (4.46)$$

where f_d is the Doppler shift in frequency, v is the relative velocity, λ is the wavelength, and θ is the angle between the transmitter and the receiver.

Rayleigh Fading Distribution

Rayleigh fading occurs when there are multiple indirect versions of the transmitted signal reaching the receiver with no dominant component signal present. This kind of fading is present when there is no Line Of Sight (LOS) component available. The distribution describes the statistical time varying nature of a flat fading channel.

The signal arriving at the receiver is the sum of multiple, independent random variables. According to the Central Limit Theorem, the sum of these random variables converges under certain conditions to a Gaussian form. The envelope of this type of random variable represents a Rayleigh distribution. The pdf of the Rayleigh distribution is given by

$$p(r) = \begin{cases} \frac{r}{\sigma^2} \exp\left(-\frac{r^2}{2\sigma^2}\right) & (0 \le r \le \infty \\ 0 & (r < 0) \end{cases} \qquad (4.47)$$

where σ is the rms value of the received voltage before envelope detection and σ^2 is the time-average power of the received signal before envelope detection. The mean value of the Rayleigh distribution is given by $r_{mean} = 1.2533\sigma$ and the variance is given by $\sigma_r^2 = 0.4292\sigma^2$. The median value of r is given by $r_{median} = 1.177\sigma$.

Statistical Models

A number of statistical models are available to describe fading channels. Some of them are Clarke's model, Jake's model, Nakagami model, two-ray Rayleigh fading model, etc. Other commonly used statistical models in the industry include Saleh and Valenzuela models, SIRCIM and SMRCIM indoor and outdoor propagation models.

Clarke's model

Assumptions:

Equal Average Amplitude - In the absence of the LOS component, the scattered components at the receiver experience similar attenuation over small distances.
Since the Doppler shift is very small, the field components of the mobile antenna are modeled as narrowband processes and for very large N, these can be modeled as Gaussian random variables. Figure 23 gives the list of the algorithm.
Spectral shape of the Doppler Spectrum: The spectrum is centered on the carrier frequency and zero outside the limits of $fc \pm fm$. For a Rayleigh Distribution, the PSD is given by

$$S_{E_z}(f) = \frac{1.5}{\pi fm \sqrt{1 - \left(\frac{f - fc}{fm}\right)^2}} \tag{4.48}$$

Algorithm

Step 1: The independent Gaussian Variables that are taken as input are complex conjugates about the center of the frequency axis that extends till $\pm fm$ where fm is the maximum Doppler Shift. This is obtained by taking FFT of random numbers generated.

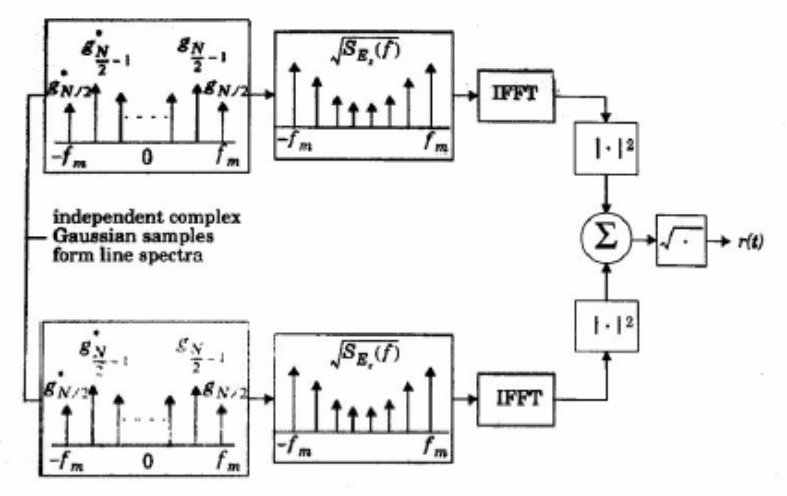

Figure 23 - Clarke's Model

Step 2: The fading spectrum $\sqrt{S_{E_z}(f)}$ is calculated using the equation given before.

Step 3: The IFFT is performed on the frequency domain signals obtained to get two time series whose squares are added and summed. The square root is then taken to obtain the simulated channel.

Ricean Distribution

When a dominant component is present along with the multipath signals thus making the signal strength considerably stronger, the distribution is said to be Ricean. The LOS component acts as this dominant component. The pdf of a Ricean distribution is given by

$$p(r) = \begin{cases} \frac{r}{\sigma^2} e^{-\frac{(r^2+A^2)}{2\sigma^2}} I_0\left(\frac{Ar}{\sigma^2}\right) & \text{for } (A \geq 0, r \geq 0) \\ 0 & \text{for } (r < 0) \end{cases} \quad (4.49)$$

where A is the peak amplitude of the dominant signal. And $I_0(\bullet)$ is the modified Bessel function of the first kind and zero-order. The parameter K is defined as the ratio between deterministic signal power and the variance of the multipath. When K tends to infinity, the pdf becomes Rayleigh, i.e., as the signal strength becomes weaker, the Ricean distribution degenerates to become a Rayleigh distribution.

For a Ricean Channel, the power spectral density is calculated using the equation

$$S_{bbE_z}(f) = \frac{1}{8\pi fm} K\left[\sqrt{1-\left(\frac{f}{2fm}\right)^2}\right] \quad (4.50)$$

Frequency Selective Channel

To simulate the multipath behavior of the channel, several rayleigh fading simulators are used in conjunction as shown in Figure 24. This produces the required attenuation and phase delay to match real-time conditions depending on gain and time delay settings.

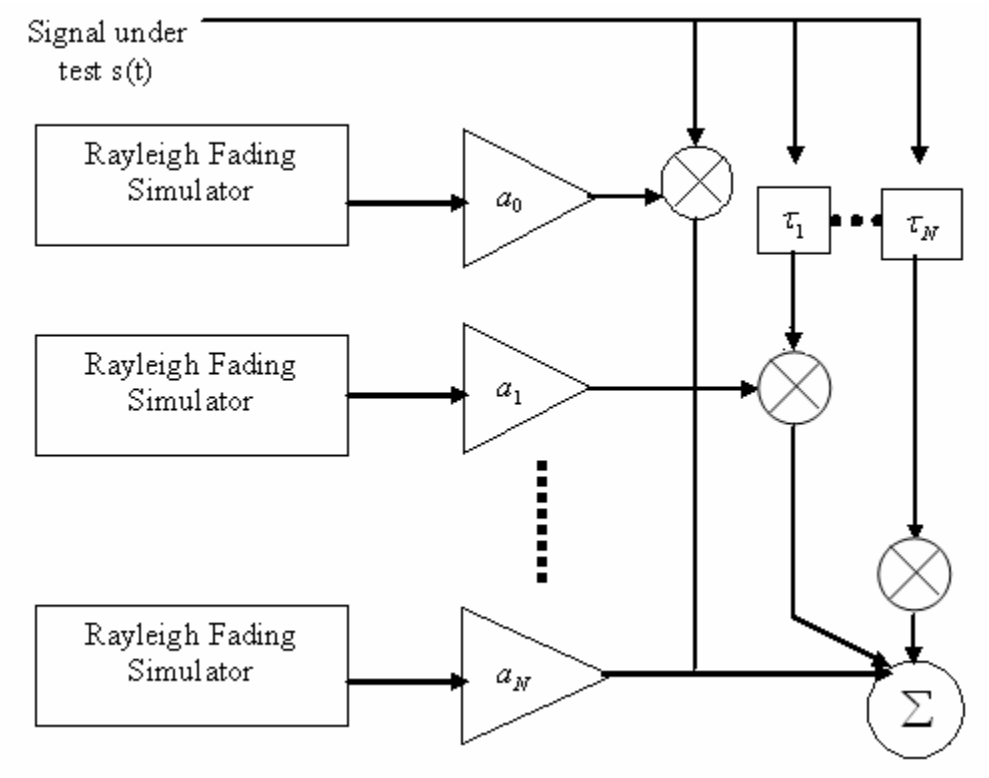

Figure 24 - Frequency Selective Fading Channel

CHAPTER 5

RESULTS AND SUMMARY

OFDM Implementation

The complex representation of the QAM modulated input symbol is given in Figure 25 and the QAM Modulated input symbols after IFFT is given in Figure 26.

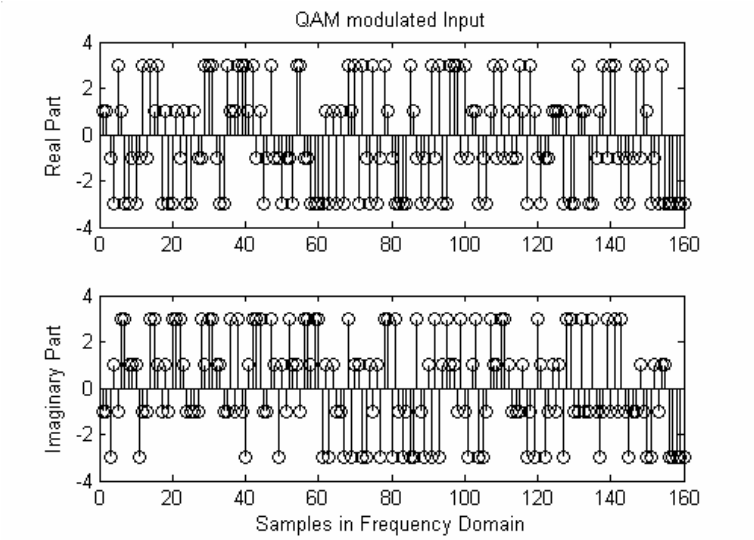

Figure 25 - Modulated Input

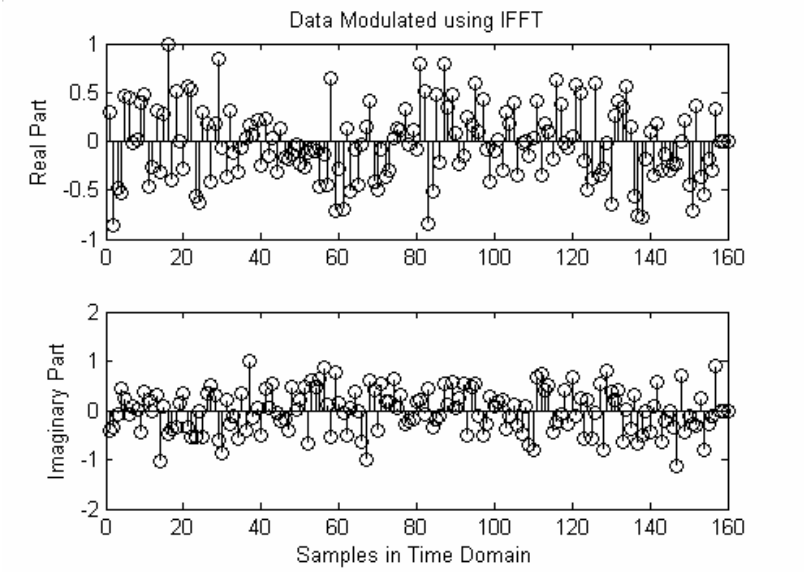

Figure 26 - Input Symbols after IFFT

The receiver section has the exact inverse of the transmitter design. The symbols after FFT are given in Figure 27.

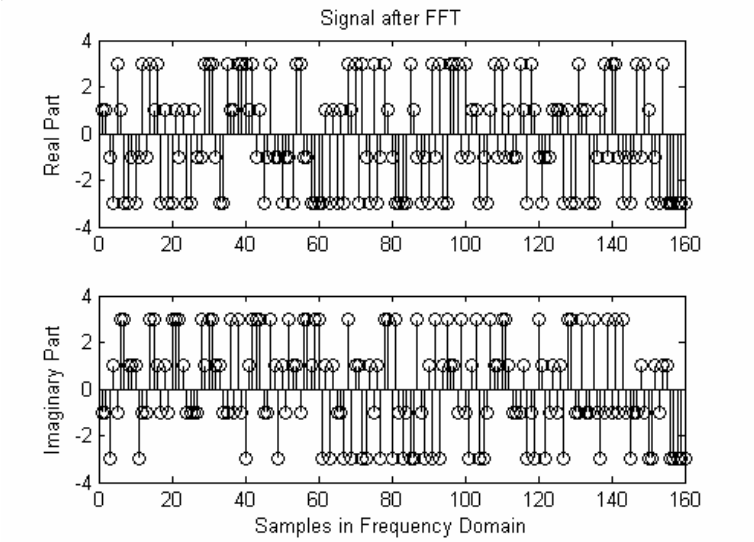

Figure 27 - Symbols after FFT in the receiver section

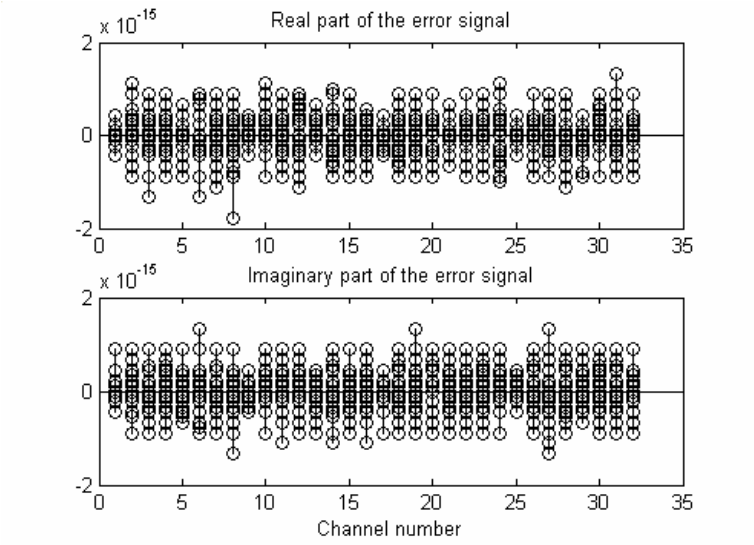

Figure 28 - Error Signal for an ideal channel

For an ideal channel, the error is negligible as shown in Figure 28. When the channel length is less than the prefix length, there is a very slight increase in error in comparison to the ideal channel response. For channel = [1 0.6 1.0 0.3 2 0.3 0.58 0.9] and prefix length = 5, the error plot across the various subchannels is given in figure 29.

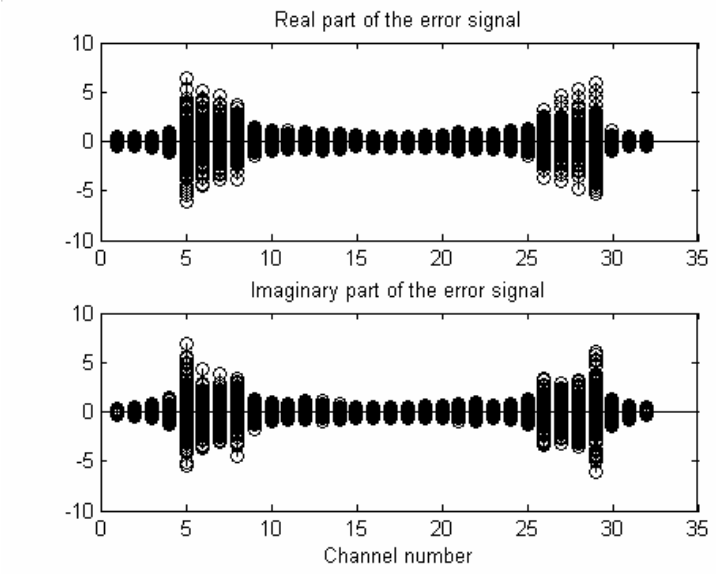

Figure 29 - Error Signal across subchannels for a non-ideal channel

To verify the performance of each subchannel, the error across the 12th subcarrier is shown in figure 30.

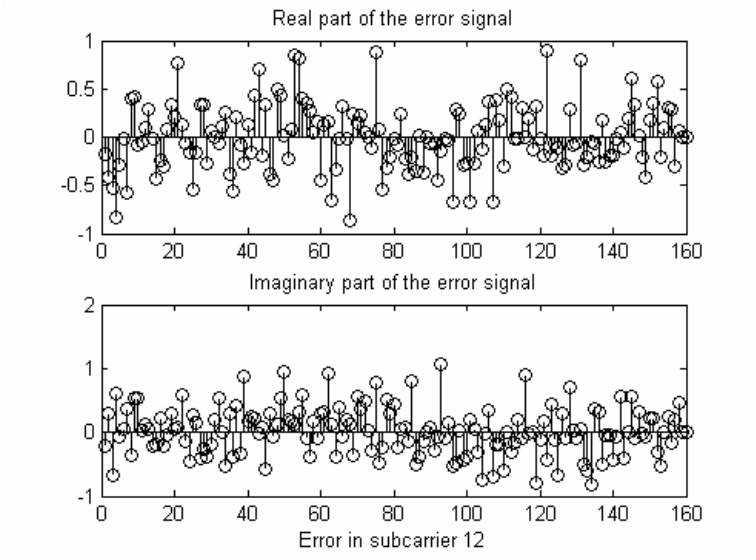

Figure 30 - Error across the 12th Subchannel

The channel impulse response is given in Figure 31.

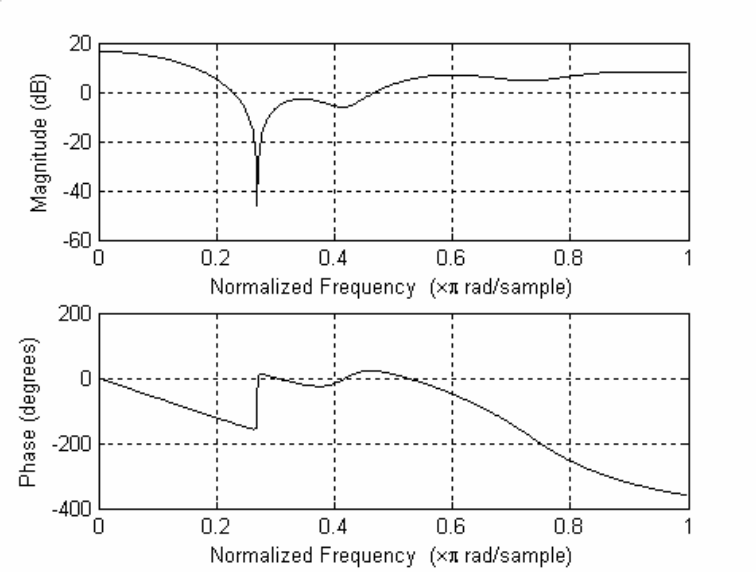

Figure 31 - Channel Impulse Response

The distribution of the output symbols is also shown in Figure 32. The addition of Additive White Gaussian noise (AWGN) to the channel also results in considerable error.

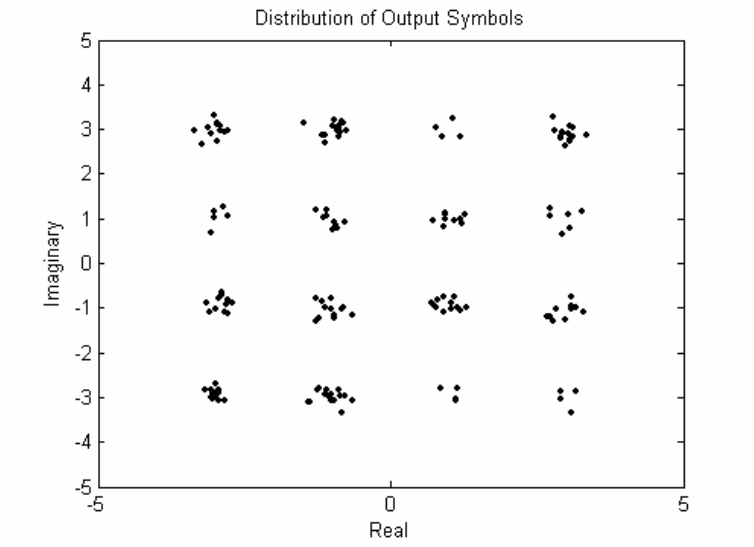

Figure 32 - Distribution of Output Symbols

MC-CDMA Implementation

Figure 33 below is the MC-CDMA transmitter output for a 3-user, 64 walsh code, QPSK modulated system. The corresponding OFDM transmitter output is in Figure 34.

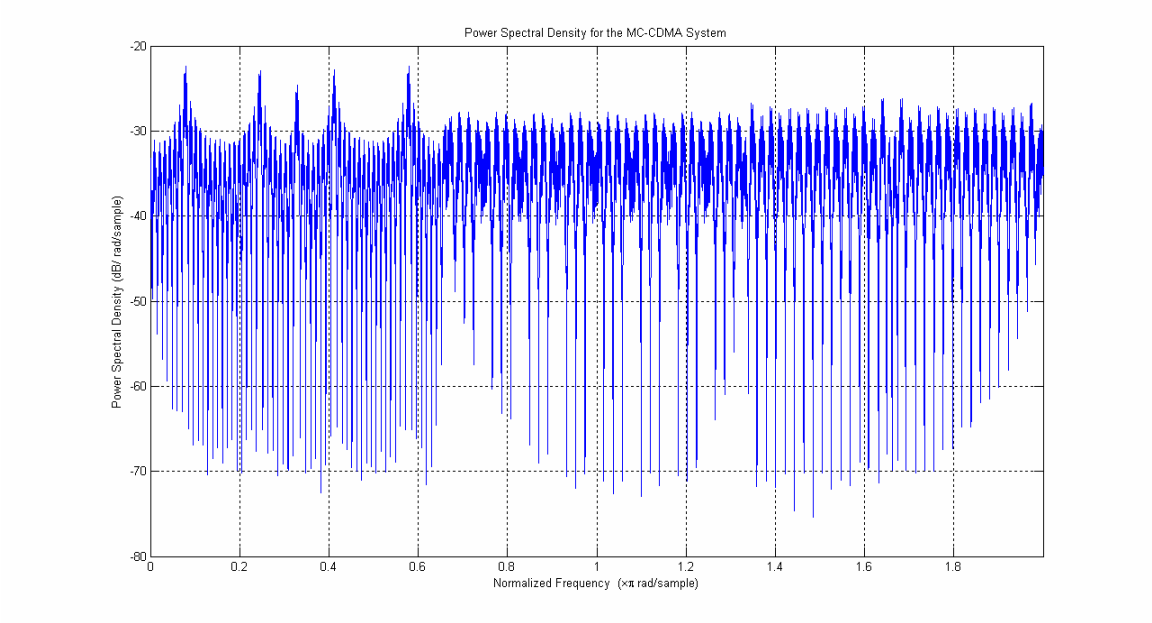

Figure 33 - MC-CDMA Transmitter Implementation

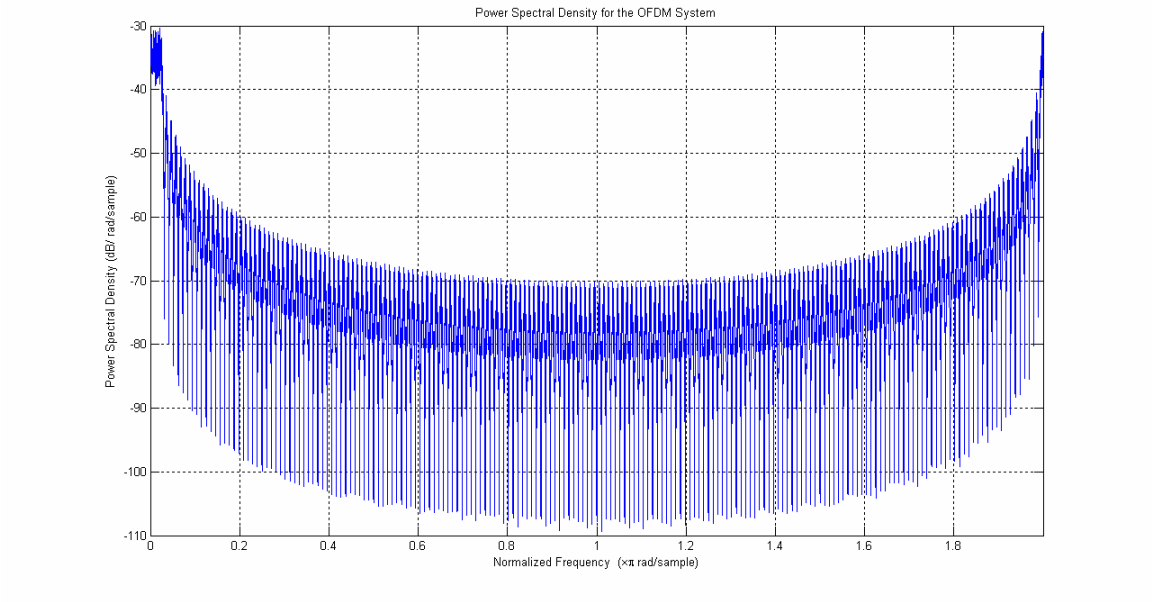

Figure 34 - Corresponding OFDM Transmitter Output

The bit error for three user MC-CDMA system is seen as negligible for an ideal channel environment is shown in Figure 35.

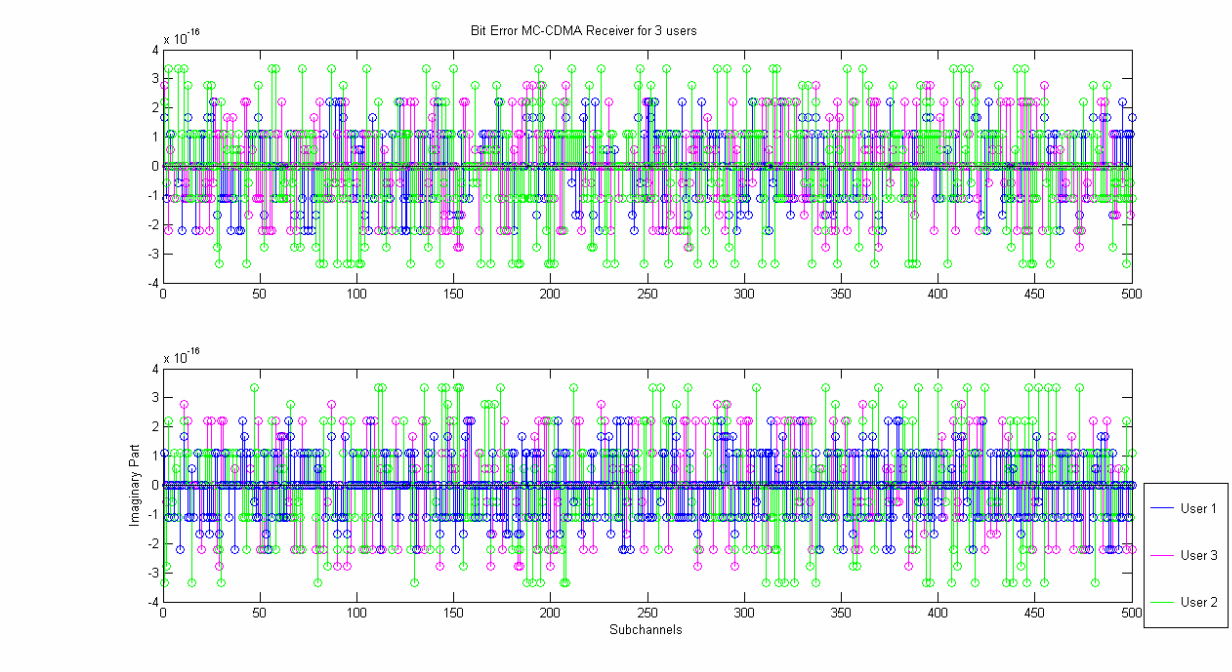

Figure 35 - Bit Error For 3-user MC-CDMA system for Ideal Channel

Channel Models - Okumura-Hata Model

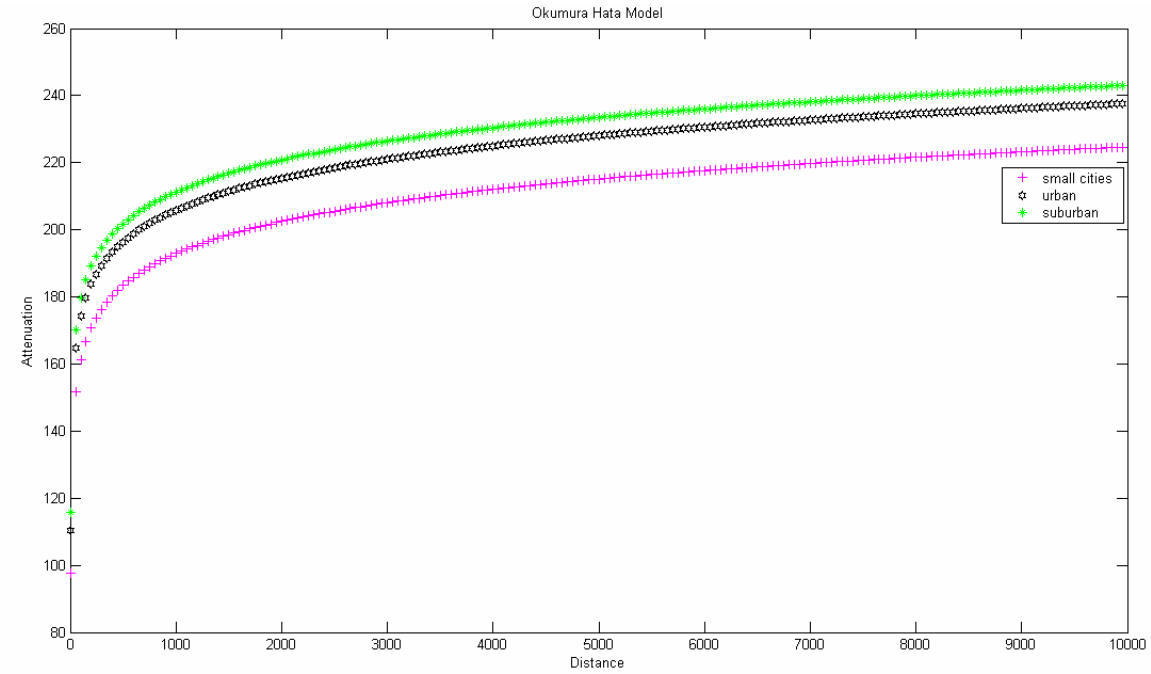

Figure 36 - Okumura Hata Model for small cities, urban and suburban areas

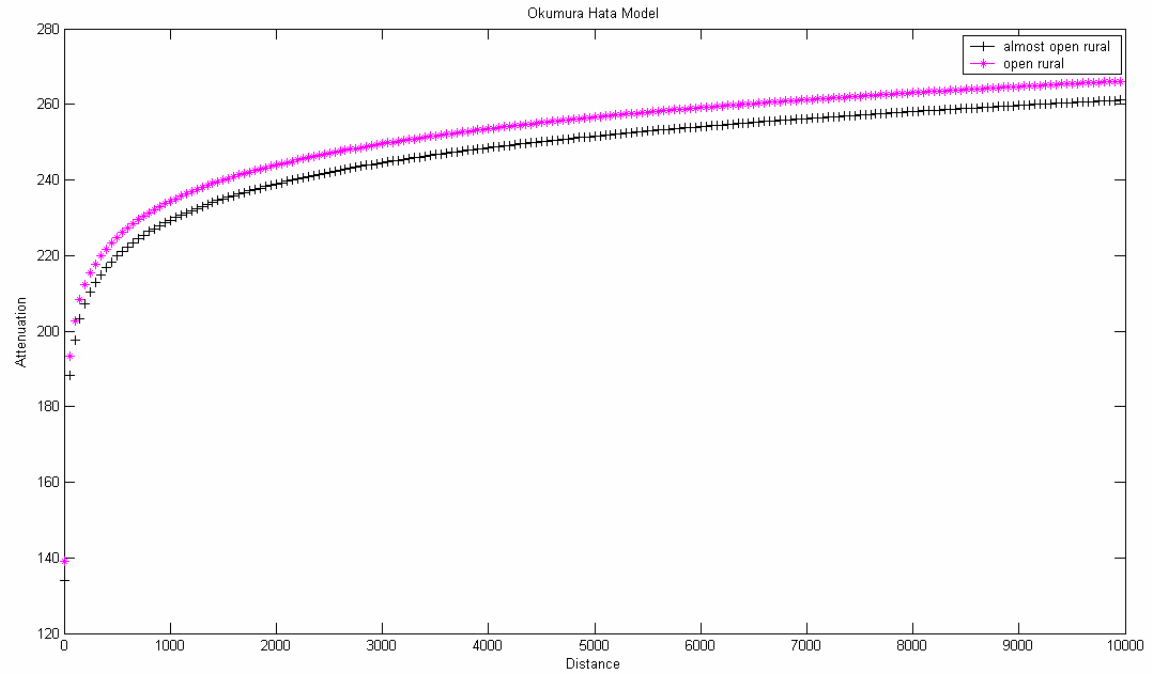

Figure 37 - Okumura Hata Model for rural areas

Longley-Rice Model

The relationship between Surface Refractivity and the Earth's effective radius is given in figure 38 and the knife-edge diffraction loss is shown in Figure 39.

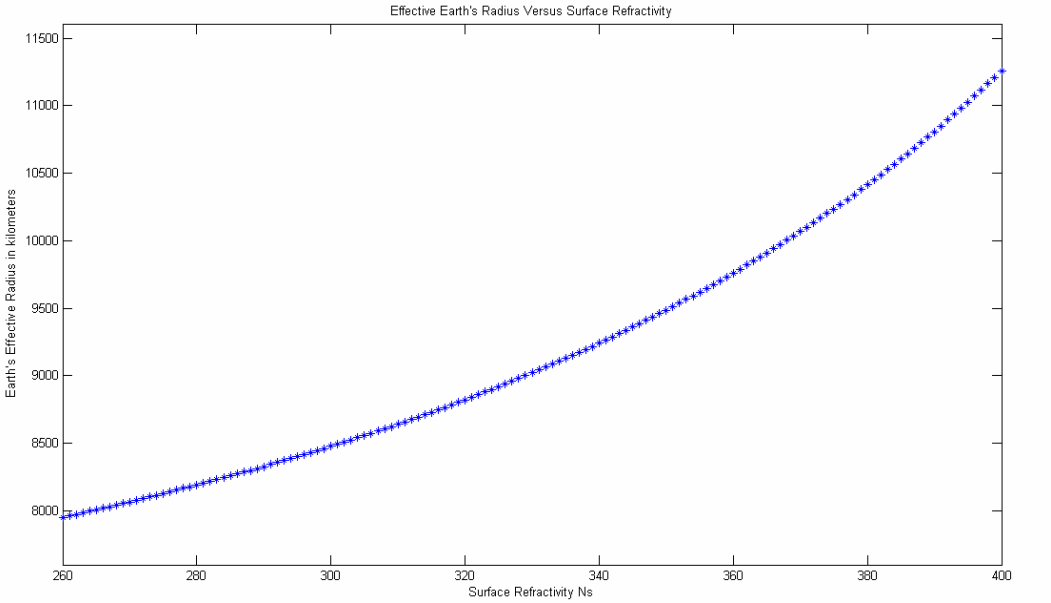

Figure 38 - Earth's Effective Radius vs Surface Refractivity

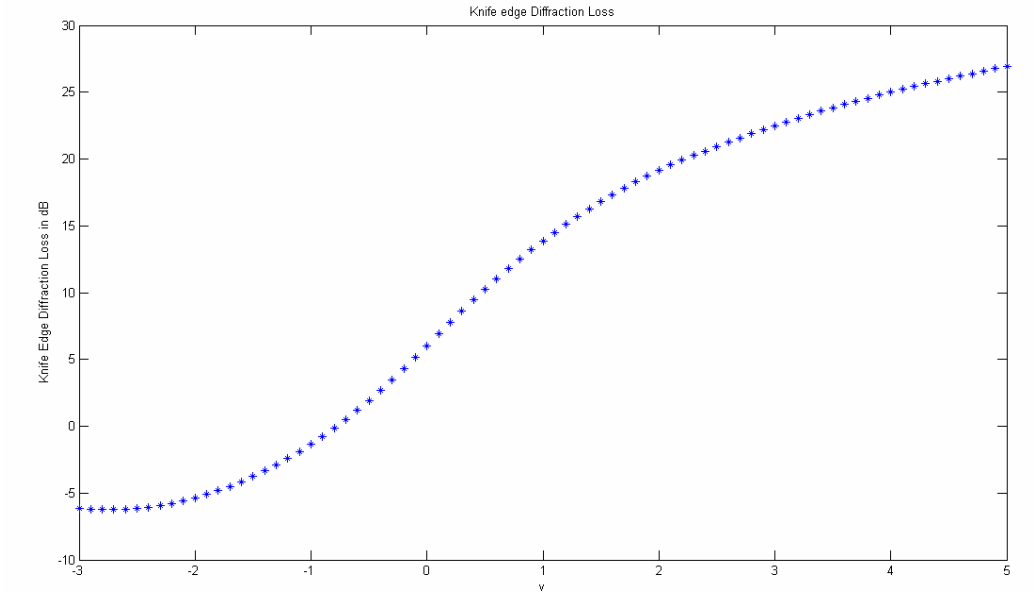

Figure 39 - Knife Edge Diffraction Loss

The relationship between angular distance and distance is plotter in Figure 40.

The free space propagation loss is shown in Figure 41.

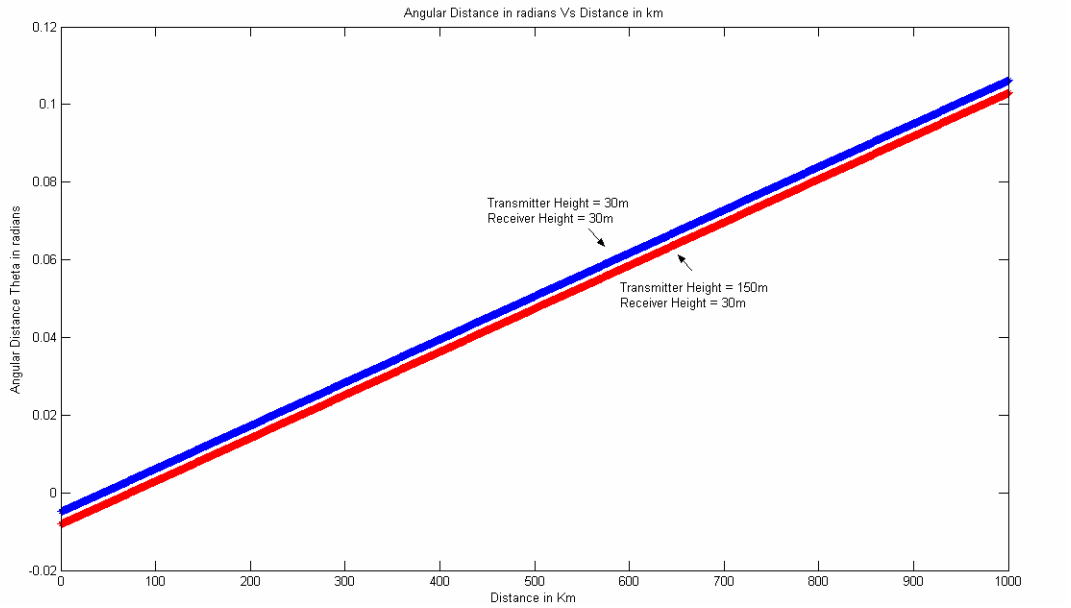

Figure 40 - Angular Distance Vs Distance

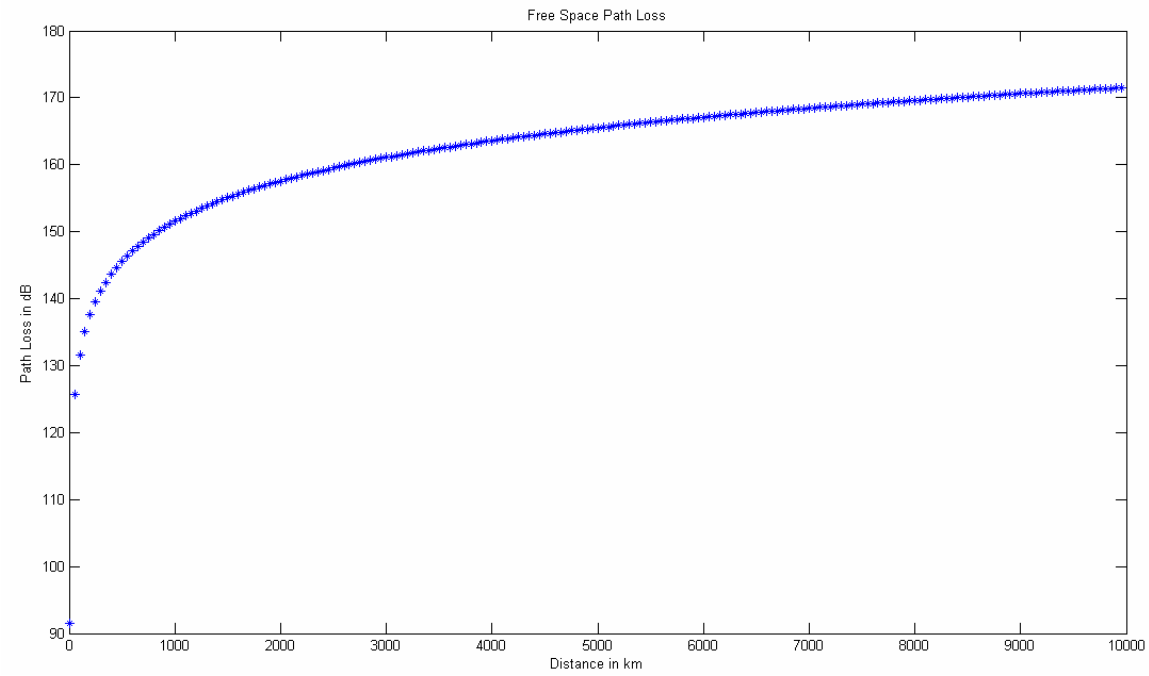

Figure 41 - Free Space Propagation Loss

The Longley-Rice Channel model is implemented and plotted in Figure 42.

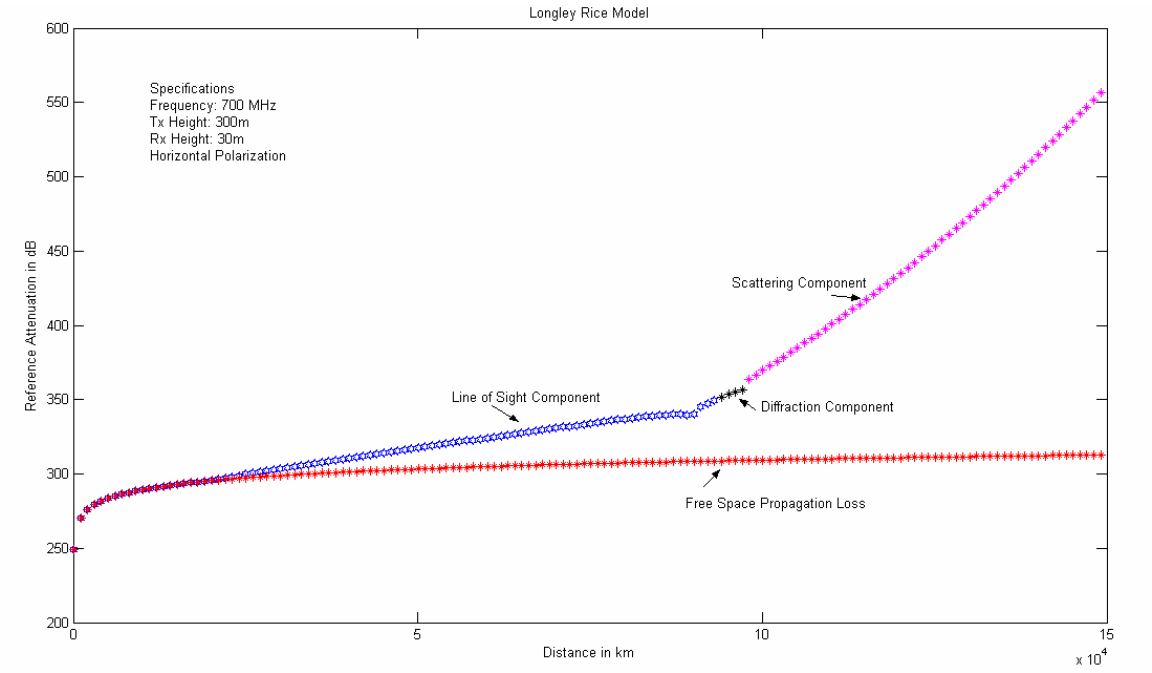

Figure 42 - Longley-Rice Model

Rayleigh Channel Model

The spectrum is centered on the carrier frequency and zero outside the limits of $fc \pm fm$ as shown in Figure 43. The fading spectrum $\sqrt{S_{E_z}(f)}$ is shown in Figure 44.

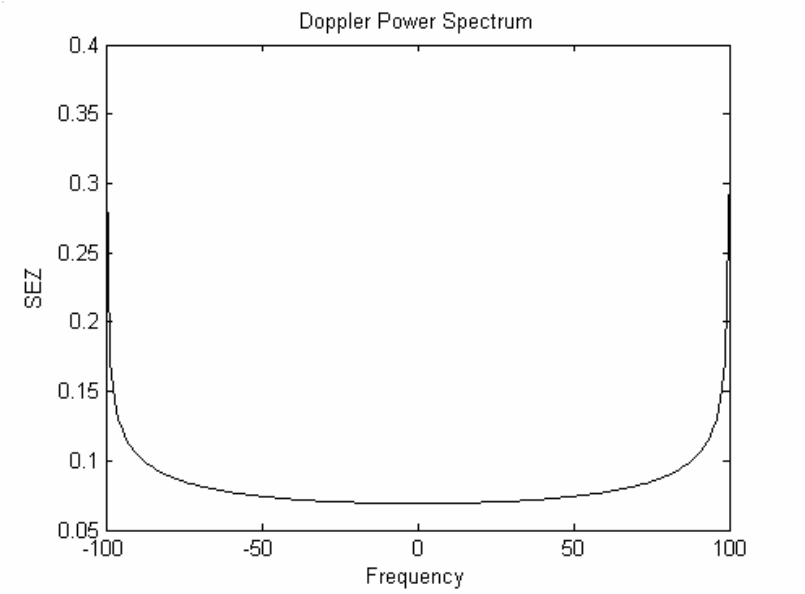

Figure 43 - Doppler Power Spectrum - Rayleigh Fading

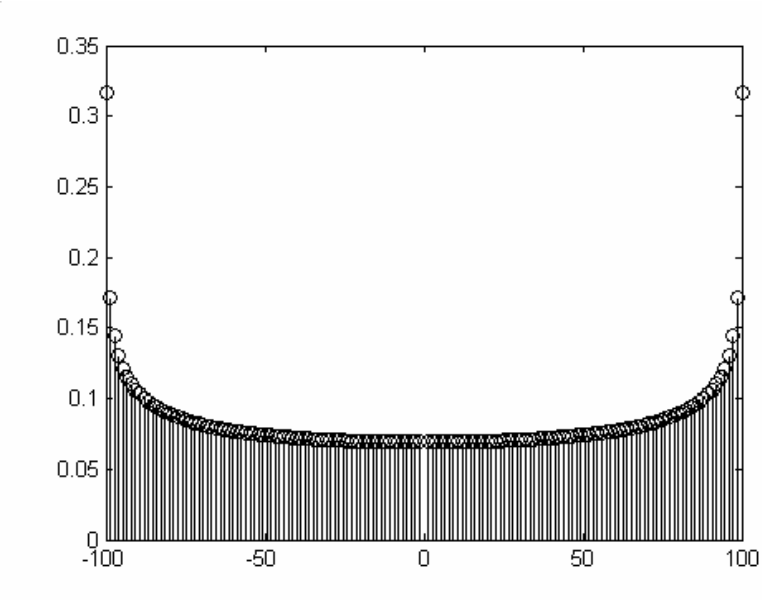

Figure 44 - Fading Spectrum

The plot of time vs signal level is given for a typical Rayleigh channel in Figure 45.

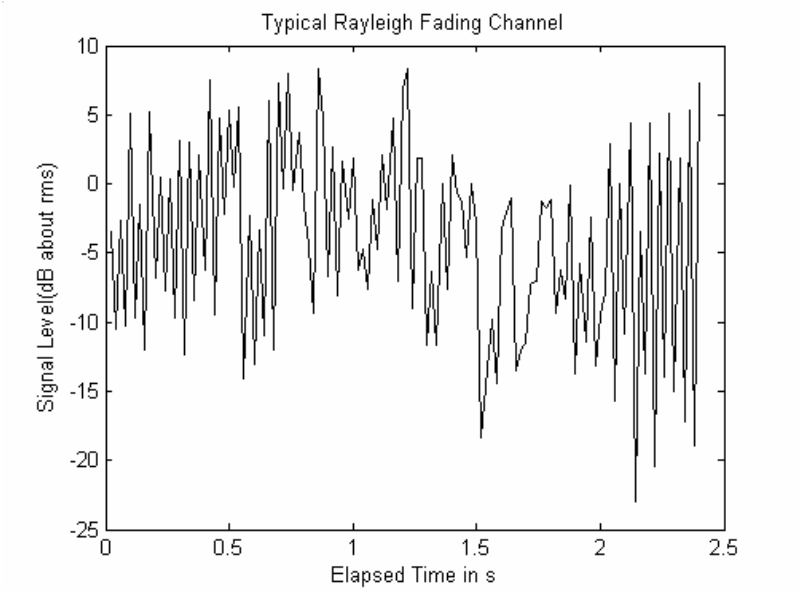

Figure 45 - Rayleigh Fading Channel

Ricean Channel Model

The received signal envelope across time is given in Figure 46.

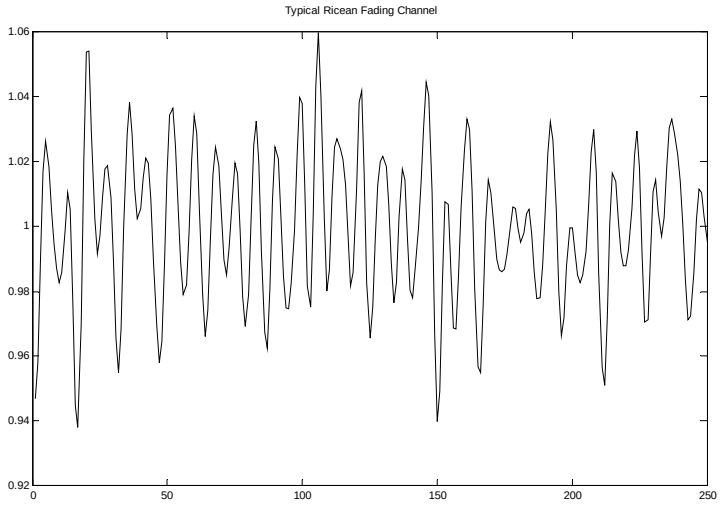

Figure 46 - Ricean Fading Channel

Summary

This thesis focuses on the study and implementation of an MC-CDMA system. It also has a comprehensive study about channel models in the wireless environment. Chapter 2 was an introduction to OFDM and CDMA and the advantages of both these modulation techniques. The OFDM system was implemented in Matlab and the performance of the system in an ideal channel and an AWGN environment was shown. Chapter 3 dealt with the study of an MC-CDMA system. Spreading of the input data was done in the frequency domain and the complete system was simulated for an ideal channel environment.

Chapter 4 is an extended study of the mobile radio channel environment. Macrocellular, microcellular and small scale fading channel environments are studied and a detailed implementation of macrocell models are done. It is shown how the Longley-Rice model takes care of diffraction, scattering and line of sight effects into consideration depending on the distance of the transmitter from the receiver.

Extensions to this work can be a study of the MC-CDMA system in the presence of macrocellular channel environments. Equalization techniques like Orthogonality Restoring Combining, Controlled Equalization, and Equal Gain Combining can be employed and the effects of the channel can be studied.

REFERENCES

[1] Theodore S. Rappaport, *Wireless Communications Principles and Practice*, Second Edition, Pearson Education, Inc., 2002

[2] Shinsuke Hara and Ramjee Prasad, "*Overview of Multicarrier CDMA*", IEEE Communications Magazine, December 1997

[3] P.L. Rice, et al, "*Transmissions Loss Predictions For Tropospheric Communication Circuits*",1967, NBS Tech Notes vol I and vol II, Available from NTIS, Nos. AD-687-820 and AD-687-821

[4] George Hufford, "*The ITS Irregular Terrain Model, The Algorithm*", National Telecommunications and Information Administration, US Department of Commerce

[5] Alexander Neskovic, Natasa Neskovic, George Paunovic, "*Modern Approaches in Modeling of Mobile Radio Systems Propagation Environment*", IEEE Communications Survey, Third Quarter 2000

[6] John G. Proakis, *Digital Communications*, McGraw-Hill, Fourth Edition, 2000

[7] http://www.awe-communications.com/Docs/WinProp_Documentation.pdf

[8] Stephen Kaiser, "*OFDM-CDMA versus DS-CDMA: Performance Evaluation for Fading Channels*"

[9] Ana Aguiar, James Gross, "*Wireless Channel Models*", Technical University Berlin, Telecommunications Network Group, April 2003.

PERMISSION TO COPY

In presenting this thesis in partial fulfillment of the requirements for a master's degree at Texas Tech University or Texas Tech University Health Sciences Center, I agree that the Library and my major department shall make it freely available for research purposes. Permission to copy this thesis for scholarly purposes may be granted by the Director of the Library or my major professor. It is understood that any copying or publication of this thesis for financial gain shall not be allowed without my further written permission and that any user may be liable for copyright infringement.

Agree (Permission is granted.)

Kruthika Ponnusamy — December 5, 2005
Student Signature — Date

Disagree (Permission is not granted.)

_____ _____
Student Signature — Date